



Hydrogeological and hydrochemical investigation of groundwater using environmental isotopes (^{18}O , ^2H , ^3H , ^{14}C) and chemical tracers: a case study of the intermediate aquifer, Sfax, southeastern Tunisia

Rahma Ayadi¹ · Rim Trabelsi¹ · Kamel Zouari¹ · Hakim Saibi² · Ryuichi Itoi³ · Hafedh Khanfir⁴

Received: 15 April 2017 / Accepted: 21 November 2017 / Published online: 19 December 2017
© Springer-Verlag GmbH Germany, part of Springer Nature 2017

Abstract

Major element concentrations and stable ($\delta^{18}\text{O}$ and $\delta^2\text{H}$) and radiogenic (^3H and ^{14}C) isotopes in groundwater have proved useful tracers for understanding the geochemical processes that control groundwater mineralization and for identifying recharge sources in the semi-arid region of Sfax (southeastern Tunisia). Major-ion chemical data indicate that the origins of the salinity in the groundwater are the water–rock interactions, mainly the dissolution of evaporitic minerals, as well as the cation exchange with clay minerals. The $\delta^{18}\text{O}$ and $\delta^2\text{H}$ relationships suggest variations in groundwater recharge mechanisms. Strong evaporation during recharge with limited rapid water infiltration is evident in the groundwater of the intermediate aquifer. The mixing with old groundwater in some areas explains the low stable isotope values of some groundwater samples. Groundwaters from the intermediate aquifer are classified into two main water types: Ca-Na-SO₄ and Ca-Na-Cl-SO₄. The high nitrate concentrations suggest an anthropogenic source of nitrogen contamination caused by intensive agricultural activities in the area. The stable isotopic signatures reveal three water groups: non-evaporated waters that indicate recharge by recent infiltrated water; evaporated waters that are characterized by relatively enriched $\delta^{18}\text{O}$ and $\delta^2\text{H}$ contents; and mixed groundwater (old/recent) or ancient groundwater, characterized by their depleted isotopic composition. Tritium data support the existence of recent limited recharge; however, other low tritium values are indicative of pre-nuclear recharge and/or mixing between pre-nuclear and contemporaneous recharge. The carbon-14 activities indicate that the groundwaters were mostly recharged under different climatic conditions during the cooler periods of the late Pleistocene and Holocene.

Keywords Arid regions · Tunisia · Groundwater mineralization · Stable/radiogenic isotopes · Groundwater recharge

Introduction

Understanding the processes and factors that control the evolution of the mineralization in aquifers over the years is an academic challenge and has important practical implications for water

resource evaluation and management in the future. The salinity of water resources has been intensively studied during the past few decades, particularly in coastal aquifers, stimulated by both scientific interest and social need (Custodio 1987; Richter and Kreitler 1993; Petalas and Diamantis 1999; Fedrigoni et al. 2001;

✉ Rahma Ayadi
ayadirahma2285@yahoo.fr

Rim Trabelsi
trabelsi.rim01@gmail.com

Kamel Zouari
kamel.zouari@enis.mu.tn

Hakim Saibi
saibi.hakim@gmail.com

Ryuichi Itoi
ittoi@mine.kyushu-u.ac.jp

Hafedh Khanfir
khanfirafedh@yahoo.fr

¹ Laboratory of Radio-Analysis and Environment, National School of Engineers of Sfax, Sfax University, Soukra Road, BP 1173, 3038 Sfax, Tunisia

² Geology Department, College of Science, United Arab Emirates University, Al-Ain, UAE

³ Department of Earth Resources Engineering, Faculty of Engineering, Kyushu University, Fukuoka, Japan

⁴ Water Resources Division of Sfax, Agriculture Ministry, Sfax, Tunisia

Vengosh 2003; Vengosh et al. 2005, 2007). In Tunisia, particularly in the south of the country, groundwater is the main water resource and is used by all the sectors. The Sfax region, located on the southeast coast of the country, has a groundwater aquifer system featuring a deep confined aquifer, an intermediate aquifer and shallow aquifers that are delimited by their respective catchment areas. Since 2000, water management authorities have been facing problems of deteriorating water quality and increasing water demands due to a rapidly increasing population and the expansion of agricultural activity. The arid climate coupled with intensive exploitation of groundwater resources is leading to water resource deficits and groundwater quality degradation (Bouchaou et al. 2008; Yangui et al. 2010). Moreover, the expansion of agricultural irrigation return, the domestic effluents and the intensive pumping have led to these difficult problems threatening the sustainable groundwater resources particularly in coastal semi-arid and arid regions. One of the most pronounced impacts of these anthropogenic processes is the increase in the nitrate concentrations derived from agricultural return flows (Hern and Feltz 1998; Hao and Change 2002) and groundwater salinization. For a better understanding of the hydrodynamic behavior, identification of the origin and the recharge mechanisms of the aquifer, carbon isotopes and stable isotopes in water have long been used as groundwater tracers (Fontes and Garnier 1979; Plummer et al. 1976; Aravena et al. 1995; Clark and Fritz 1997) in conjunction with chemical data. ^{14}C is the most reliable chronometer of moderately old groundwater (5 ± 30 ka), although corrections should account for water–rock interactions. Stable isotopes have been used to identify possible recharge areas and mixing within aquifer systems (Trabelsi et al. 2009; Zouari et al. 2011). However, in regional studies, interpretations of stable isotope data can become very complex because their input functions vary according to a number of different factors, including elevation, precipitation amount, continentality and long-term climate change (Clark and Fritz 1997; Dansgaard 1964; Rahoui and Koshel 1980). Previous hydrogeological studies of this region (El Batti and Andrieux 1977; Beni Akhy 1994; Maliki 2000; Fedrigoni et al. 2001; Trabelsi et al. 2005) have shown that the Sfax plain contains two main aquifers: a shallow aquifer (Plio-Quaternary) overlying a deep aquifer (Miocene) that is overexploited. Recently, several hydrogeological studies (Gassara and Ben Marzouk 2009; Hchaichi 2008; Ben Ali 2011; Hchaichi et al. 2013) had demonstrated the existence of an intermediate aquifer in the detrital Mio-Pliocene deposits. The isotopes commonly employed in groundwater investigations are the stable isotopes of the water molecule, ^2H and ^{18}O , and the radioactive isotopes tritium and carbon-14. Groundwater resources in the southern part of Tunisia play an important role in providing water for domestic, industrial, and agricultural uses. In the present work, combined chemical and isotopic approaches have been developed to study the groundwater from the Sfax aquifer system by identifying groundwater flow paths and recharge areas, and revealing the main processes controlling the

evolution of water for achieving proper management and protection of these important resources.

Geological and hydrogeological setting

The Sfax region, located in the east coast of Tunisia, is the second biggest urban area after Tunis. The Sfax basin is bounded by the Mediterranean Sea in the eastern part. The western part is occupied by the north–south (N–S) axis (Jebel J. Gouleb: 736 m, J. Zebbouz: 541 m, J. Boudinar: 716 m, J. Goubrar: 622 m, J. Krechem el Artsouma: 655 m) and the southern by the Skhira area (Fig. 1). The studied area has a semi-arid Mediterranean climate with an average annual precipitation and temperature of 226 mm and 19 °C, respectively (CRDA Sfax 2015). The geology of the area was investigated by Castany (1953), Burollet (1956) and Zébidid (1989). The Sahel in the Sfax area is characterized by a monotone topography of small hills, separated by wide basins occupied by sabkhas. The geology of the study area is dominated by outcrops of Mio-Pliocene and Quaternary deposits. Most of the outcrops were controlled by the major tectonic phases that have occurred in the region (Ben Akacha 2001). The study area contains long-wavelength anticlines with relief of less than 200 m (Belgacem et al. 2010). The lithology includes the Souar Formation, which is attributed to the Eocene age and is formed by marine sediments (Bouaziz 1994). The Oligocene sediments feature a lower marine unit and an upper continental sandy unit. The Miocene thick deposits are composed of an alternation of clay, sand and sandstone. These deposits are divided into three units from the bottom to the top (Tayech 1984): the Ain Ghrab Formation (Burdigalian, lower Miocene), consisting primarily of limestone interbedded with gypsum; the Oum Douil Formation (Langian to Tortonian: upper Miocene), containing variable proportions of silt and clay; and the Segui Formation (Messinian), consisting of alternating continental sand, silt and clay. Pliocene marl deposits discordantly overlie the older formations. The regional superficial aquifer system is located in the upper Miocene, Pliocene and Quaternary deposits mainly formed by sands and silty clays. This multilayered aquifer is interbedded with semi-permeable layers (Hchaichi et al. 2013; Ayadi et al. 2016). The aquifer system of Sfax is composed of three aquifers.

The shallow aquifer

The shallow aquifer is an unconfined superficial unit located in the Quaternary and Mio-Pliocene deposits, comprising sand and silty clay layers that are separated by sandy clays (Hajjem 1980; Maliki 2000). Its thickness varies from 8 to 60 m. The substratum of the reservoir is composed of a clayey-sandy unit of continental origin. It is characterized by alternations of unrefined natural sands and conglomerates, with beds of red sandy marls and clays. The main direction of groundwater flow is from NW to SE (Takrouni et al. 2003). The aquifer is recharged by direct

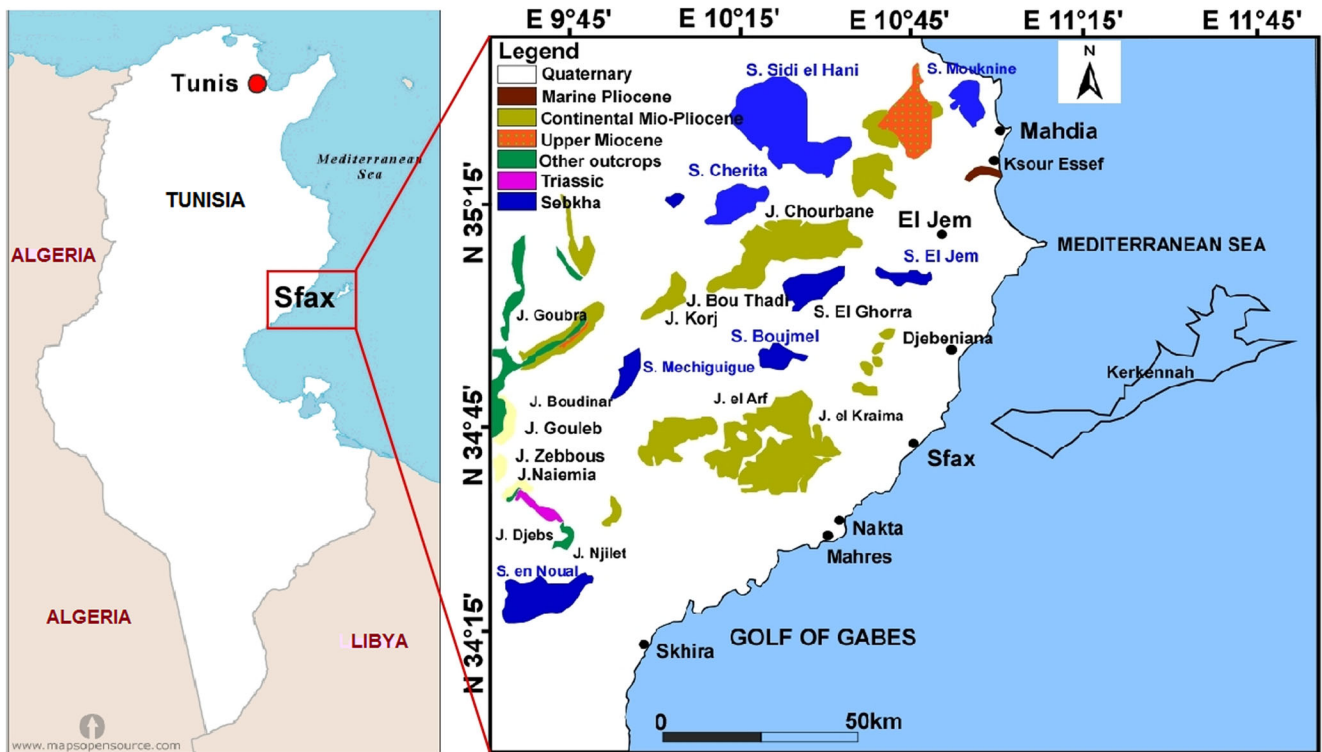


Fig. 1 Location and geological map of the study area, including Sebkhha (S.) and Jbel (J.) (From the geological map of Tunisia at 1/500,000)

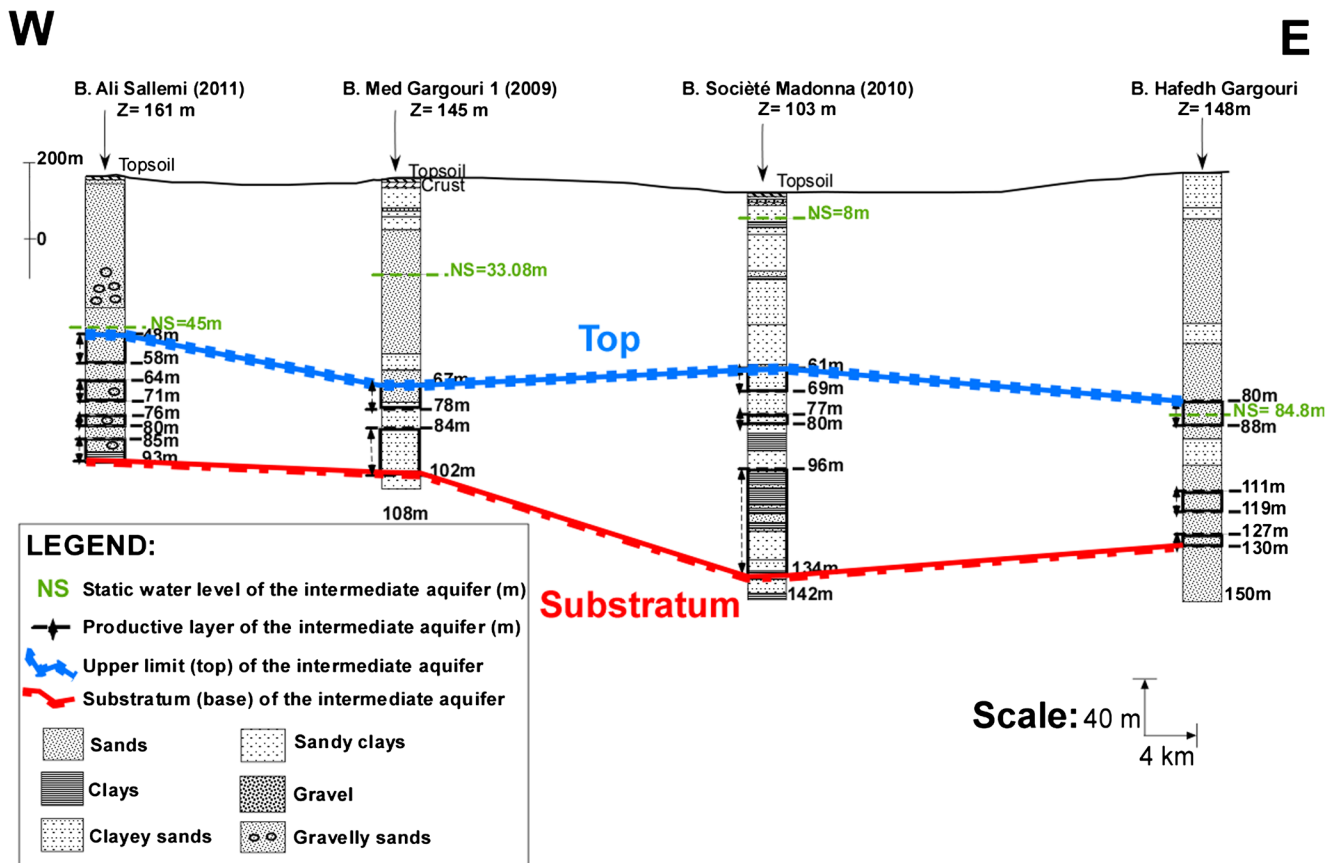


Fig. 2 Hydrogeological cross-section of the intermediate aquifer system (Ayadi 2017)

infiltration through the permeable layers of sand and sandy clay with permeability values between 4×10^{-6} and 68×10^{-4} m/s (Ben Brahim et al. 2011). Based on pumping tests, the transmissivity was estimated to 1.5×10^{-3} m²/s (Maliki 2000).

The intermediate aquifer

The intermediate aquifer (Fig. 2), situated between the shallow and deep aquifers, has been identified at depths between 70 and 200 m. It consists of Pliocene and Quaternary sand and sandy clay deposits. It is characterized by its multi-layered feature, composed of several units of detrital sediments separated by clay-rich strata, producing heterogeneity in this aquifer. As shown in Fig. 2, the intermediate aquifer presents significant lateral and vertical variation in facies and in thickness. The measured transmissivities are in the range of 1×10^{-4} to 4.32×10^{-3} m²/s (Hchaichi 2008, Hchaichi et al. 2013). The water resources of the middle aquifer were estimated to be 11.3 Mm³/year (CRDA Sfax 2015). A piezometric map of the intermediate aquifer in Sfax (Fig. 3) was conducted using the piezometric measurements of 28 boreholes and 5 piezometers taken during 2014 (CRDA Sfax 2015). The piezometric mapping was performed with the aid of the ArcMap 10.3 program with natural neighbor interpolation. This map shows that the main groundwater flow direction is NW–SE towards the Mediterranean Sea, which forms the natural discharge area. Indeed, the highest values are found in the north and northwest and decrease towards the south and

southeast. This may indicate that the recharge of the intermediate aquifer of Sfax occurs in the northwestern and western parts.

Miocene deep aquifer

The Miocene deposits host the deepest aquifer. It constitutes a primordial source for the water supply of the region. This aquifer is located at depths between 200 and 700 m, its average thickness is 150 m, and it covers an area of approximately 15,000 km². It is logged as sand and sandstones interbedded with clay. The pumping tests show that the transmissivity values vary between 0.123×10^{-3} and 130×10^{-3} m²/s with an average of 23.32×10^{-3} m²/s. The maximum thickness is observed in the central part of the basin and decreases towards the Skhira region to be minimal at the Kerkennah Island (Trabelsi et al. 2006). The groundwater flow direction is generally towards the southeast, implying discharge to the Mediterranean Sea, the natural outlet (Trabelsi et al. 2006).

Methodology, groundwater sampling and analytical procedures

The sampling campaign (Fig. 4) was carried out on the Sfax Plain from September 2012 to May 2016. Samples from 116 sites were collected from deep wells of the intermediate aquifer whose depth varied from 60 to 450 m and were characterized using

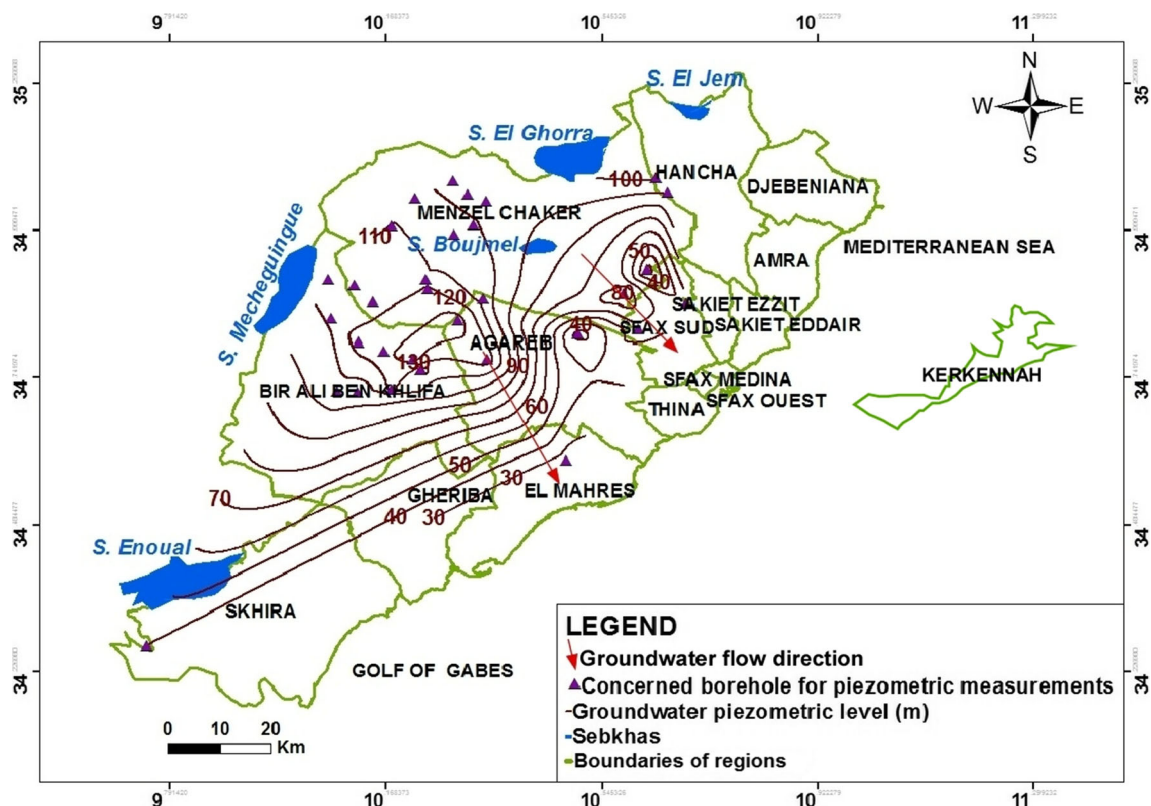


Fig. 3 Piezometric map of the intermediate aquifer

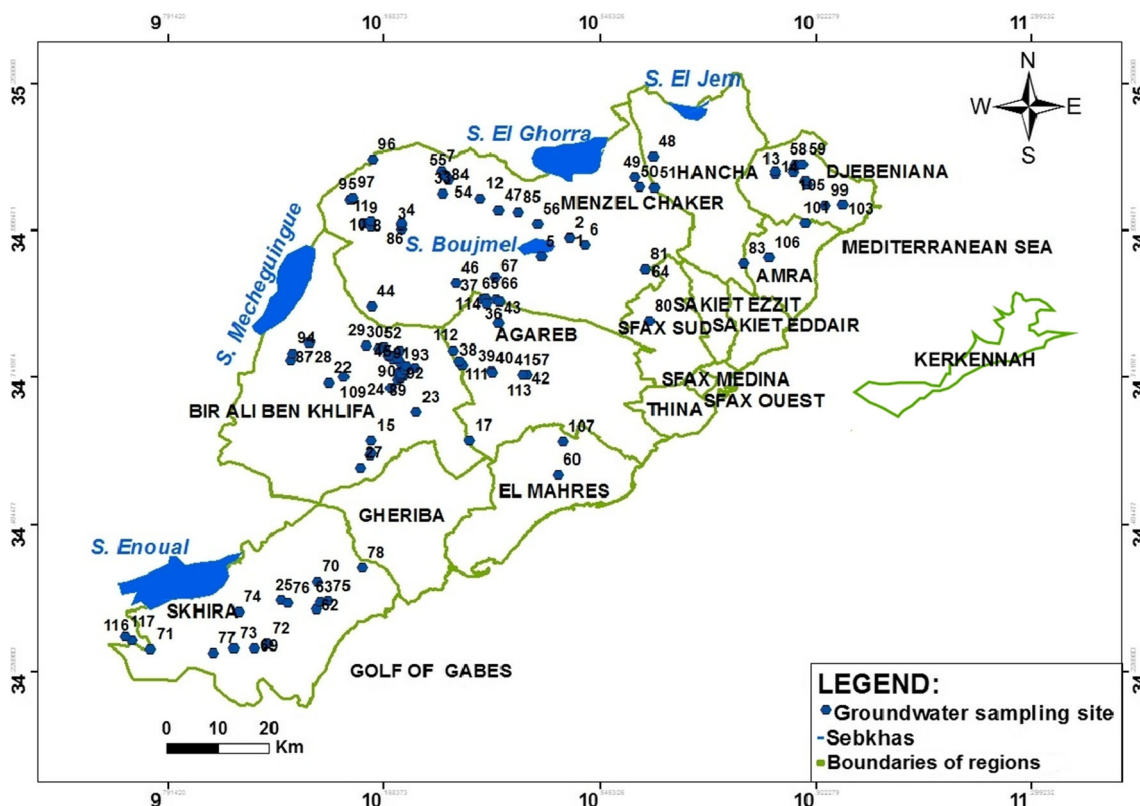


Fig. 4 Sampling sites of groundwater from the intermediate aquifer of Sfax

chemical and isotope analyses. It was a one-time sampling for each analyzed groundwater; therefore, no seasonal effect can be indicated. Water temperature, electrical conductivity (EC) and pH values were determined in the field. Bicarbonate content was measured by titration with 0.1 N-HCl. Chemical and isotopic analyses were conducted at the Laboratory of Radio-Analyses and Environment of the National Engineering School of Sfax (ENIS, Tunisia). The major cation (Ca, Mg, Na and K) and anion (Cl, SO₄ and NO₃) concentrations were determined by liquid-ion chromatography (ILC). The chromatograph was equipped with IC-Pak TM CM/D columns for cations, using EDTA and nitric acid as eluent, and CI SUPER-SEP columns for anions, using phthalic acid and acetonitrile as eluent. The ionic balance is within ±5%. An analysis is considered valid if the value of its ionic balance is within ±5%. These values guarantee the reliability of the chemical results. Isotopic analysis was performed with a LGR DLT 100 Laser Absorption Spectrometer and the δ¹⁸O and δ²H results are reported in the usual δ notation relative to the Vienna Standard Mean Ocean Water (V-SMOW) standard, where $\delta = [(R/R_{V-SMOW}) - 1]/1,000$ (*R* represents either the ¹⁸O/¹⁶O or the ²H/¹H ratio of the sample, and *R_{V-SMOW}* is the ¹⁸O/¹⁶O or ²H/¹H ratio of the V-SMOW standard; Coplen 1996).

The precisions of the measurements for stable isotopes analyses were ±0.1 and ±1‰ for δ¹⁸O and δ²H, respectively. In total, 64 samples were selected for tritium content analysis using the electrolytic enrichment and liquid scintillation techniques (Taylor 1976). The ³H concentration is expressed in tritium units

(TU). One TU is defined as the isotope ratio ³H/¹H = 10⁻¹⁸. Fourteen groundwater samples were analyzed for carbon-14 dating activity. Precipitation of BaCO₃ from groundwater samples was carried out in the Laboratory (ENIS, Tunisia). Radiocarbon activities were determined by using benzene synthesis and liquid scintillation spectrometry (Fontes 1971; Stuiver and Polach 1977). The results are reported as percent of modern carbon (pmc) with an analytical uncertainty of ±1 pmc. The geochemical program PHREEQC software, version 2.10.0.0 (Parkhurst and Appelo 1999), with the thermodynamic dataset wateq4f.dat, was employed to evaluate the saturation status of minerals in well water samples. The saturation index (SI) indicates the potential for chemical equilibrium between water and minerals and the likelihood of water–rock interactions (Wen et al. 2008). The chemical analyses are given in mg/L. The formula used for converting from mg/L to meq/L is provided here for the interpretation of some diagrams: concentration (meq/L) = concentration (mg/L)/molar mass × ionic charge of the chemical element.

Results and discussion

Hydrochemistry

The major ion concentrations and physico–chemical characteristics of the analyzed water samples are presented in Table 1. The temperature of groundwater samples from the

Table 1 Physico-chemical characteristics and chemical composition of the groundwater samples

Site/sample No.	Sample location	Sample name	Cl (mg/L)	NO ₃ (mg/L)	SO ₄ (mg/L)	HCO ₃ (mg/L)	Na (mg/L)	K (mg/L)	Mg (mg/L)	Ca (mg/L)	TDS (mg/L)	EC (µS/cm)	T (°C)	pH	Borehole depth (m)
1	Menzel Chaker	Hafedh Jarraya 1	3,732.10	76.50	2,798.40	164.70	1,991.11	27.03	583.27	730.49	10,106	4.58	21.70	7.08	180
2	Menzel Chaker	Hafedh Jarraya 3	856.95	211.85	2,247.10	152.50	574.29	83.02	209.28	646.20	5,009	6.14	21.70	6.97	196
3	Menzel Chaker	Med Chabchoub 1	157.50	50.82	1,255.86	250.10	258.76	9.20	114.43	302.92	2,481	2.98	20.40	7.05	100
4	Menzel Chaker	Med Chabchoub 2	360.96	52.32	2,054.52	103.70	323.23	10.73	179.52	535.67	3,672	4.16	22.30	7.09	100
5	Menzel Chaker	Mahdi Jarraya	2,128.84	62.09	2,775.64	128.10	1,202.09	20.08	362.80	756.46	6,890	9.00	21.80	7.09	84
6	Menzel Chaker	Nabiha Charfi	1,492.35	33.05	1,489.10	195.20	814.80	14.29	205.20	495.13	4,772	6.80	22.20	7.00	164
7	Menzel Chaker	OTD Essatema	368.97	32.94	1,131.87	305.00	580.42	4.25	85.96	133.33	2,491	3.53	24.00	7.25	123
8	Menzel Chaker	Tarak Fourati	553.75	47.05	2,527.70	164.70	729.60	15.11	214.42	420.19	4,672	5.59	22.70	7.17	95
9	Menzel Chaker	Zied Fourati 2	662.64	58.08	2,805.54	164.70	882.85	19.25	243.54	480.98	5,349	6.15	22.50	7.16	98
10	Menzel Chaker	Enna Fourati 2	554.65	48.40	2,458.70	170.80	727.93	12.80	204.18	416.68	4,648	5.42	22.50	7.21	67
11	Menzel Chaker	Zied Fourati 3	445.70	96.55	2,639.75	164.70	679.44	13.74	245.36	483.01	4,865	5.42	22.20	7.13	88
12	Menzel Chaker	Hafedh Jarraya 2004 (Attoura)	3,632.70	10.00	2,711.30	103.70	2,079.70	0.00	504.60	621.90	9,664	13.32	23.30	6.94	130
13	Djebeniana	Med Dziri	430.64	130.68	1,398.56	91.50	271.20	17.56	110.96	542.80	3,297	6.74	21.80	6.74	84
14	Djebeniana	Nasr Eddeli	352.40	83.84	1,532.12	97.60	171.20	13.52	95.00	677.60	3,135	6.82	22.30	6.82	99
15	Chaffar	Forage PF 83	907.55	28.60	1,738.15	158.60	736.70	0.00	170.25	467.00	4,508	7.75	-	7.75	83
16	Chaffar	Forage PF 100	593.24	40.00	1,621.20	207.40	763.32	7.72	102.96	263.12	3,411	7.51	-	7.51	100
17	Bir Ali Ben Khalifa	Chaal 1	28.05	24.89	98.19	305.00	94.41	0.00	20.94	56.31	628	0.75	22.30	6.49	71
18	Bir Ali Ben Khalifa	Forage Nejah haj Itanef	52.92	30.88	213.28	347.70	208.13	0.00	16.42	45.43	838	1.74	19.10	7.21	96
19	Bir Ali Ben Khalifa	F. Mourad Ellili	451.20	29.20	1,661.96	195.20	735.32	0.00	94.36	186.20	3,314	4.50	21.80	7.38	107
20	Bir Ali Ben Khalifa	F. Mostfa Belhaj Itanef	17.62	18.84	79.03	286.70	68.07	1.21	21.42	64.05	540	0.64	-	7.70	-
21	Bir Ali Ben Khalifa	Ahmed Zribi	232.83	14.52	1,012.41	268.40	479.58	0.00	59.74	130.61	2,017	2.73	23.80	6.66	75
22	Bir Ali Ben Khalifa	Ali Chouket	504.32	18.32	1,547.88	170.80	695.47	13.27	114.92	227.03	3,390	4.38	24.30	7.15	103
23	Bir Ali Ben Khalifa	Sahbi Jrirjir	535.72	28.16	1,561.36	170.80	623.19	0.00	144.56	330.98	3,352	4.06	21.60	6.77	62
24	Bir Ali Ben Khalifa	Mohamed Zribi (2010)	374.88	14.36	1,861.48	170.80	696.97	0.00	117.15	243.16	3,394	4.17	23.40	6.79	73
25	Skhira	Abdellatif Frikha	923.30	37.85	2,124.85	109.80	658.64	29.78	162.84	614.31	4,569	5.46	15.90	5.85	97
26	Bir Ali Ben Khalifa	Forage Nabihia Kolsi	348.24	23.31	1,545.12	219.60	626.91	0.00	90.27	245.52	2,970	5.80	18.90	7.31	85
27	Bir Ali Ben Khalifa	F. Ali B.Salem	1,027.10	41.80	2,054.20	152.50	895.35	13.00	188.25	522.10	4,450	5.67	21.80	7.35	83
28	Bir Ali Ben Khalifa	F. Med Khaled Ellouze	667.55	38.95	2,636.60	128.10	693.30	9.80	169.55	551.85	5,293	6.88	22.90	6.52	145
29	Bir Ali Ben Khalifa	F. Ali Abouda	2,288.20	64.60	2,730.80	97.60	1,244.60	0.00	408.20	799.10	8,084	9.56	-	7.76	118
30	Bir Ali Ben Khalifa	F. Jilani Itanef	426.45	2.15	2,538.30	146.40	839.45	0.00	176.95	348.85	4,975	5.72	-	8.11	127
31	Bir Ali Ben Khalifa	F. Moez Mezghani	242.25	19.65	1,075.25	359.90	510.88	0.00	68.03	121.90	2,368	3.14	-	8.09	110
32	Bir Ali Ben Khalifa	F. abdelhafith bougueffia	107.10	32.10	578.74	378.20	357.84	2.60	34.84	79.46	1,430	1.92	-	7.81	70
33	Menzel Chaker	F. Limaya	1,887.60	66.00	1,735.20	146.40	823.80	31.60	342.60	767.60	6,400	7.63	-	7.73	110
34	Bir Ali Ben Khalifa	Mourad Nouri	283.78	33.36	841.24	256.20	455.04	0.00	65.92	150.26	1,900	2.57	-	7.94	100
35	Menzel Chaker	F. Haj Gacem	414.28	73.64	2,483.16	115.90	546.40	4.00	204.04	554.60	4,396	6.70	-	7.50	136
36	Agareb	Othmen Maaalej 1	128.05	26.45	3,254.45	176.90	409.75	34.95	259.60	759.15	4,858	4.32	-	7.23	114
37	Agareb	Othmen Maaalej 2	232.20	22.80	1,181.76	176.90	461.12	4.56	69.04	240.28	2,242	2.91	-	7.45	110
38	Agareb	Itaif Mezghanni	1,982.20	43.00	2,999.10	128.10	1,452.20	15.90	287.80	913.20	7,399	9.23	-	7.45	110
39	Agareb	Zouhir Miziou 1	658.95	125.20	2,514.90	195.20	931.60	18.95	175.75	538.75	4,856	5.26	-	7.42	133
40	Agareb	Zouhir Miziou 2	762.55	30.95	2,437.85	189.10	998.40	0.00	198.75	374.95	5,098	5.97	-	7.43	125
41	Agareb	Mustapha Frikha (1)2013	1,411.64	0.00	1,076.56	164.70	764.12	20.08	140.80	343.16	3,579	6.26	-	7.50	160
42	Agareb	Mustapha Frikha (2)2013	1,092.60	0.00	969.00	154.20	690.40	0.00	110.00	400.20	3,472	-	-	-	242
43	Agareb	Sfax Zetiana	368.00	44.32	2,122.44	170.80	571.76	0.00	150.32	336.16	3,511	6.10	-	7.40	142
44	Bir Ali Ben Khalifa	Hedi Ellouze	184.03	29.30	1,201.78	134.20	366.33	8.58	90.25	212.55	2,407	2.84	-	7.85	160

Table 1 (continued)

Site/sample No. (Fig. 4)	Sample location	Sample name	Cl (mg/L)	NO ₃ (mg/L)	SO ₄ (mg/L)	HCO ₃ (mg/L)	Na (mg/L)	K (mg/L)	Mg (mg/L)	Ca (mg/L)	TDS (mg/L)	EC (µS/cm)	T (°C)	pH	Borehole depth (m)
45	Bir Ali Ben Khalifa	Forage Mahmoud Mezghanni	134.44	23.52	962.06	237.90	522.88	0.00	42.58	86.78	2,001	3.50	–	7.30	103
46	Menzel Chaker	Hsan Maktouf	536.44	112.96	1,381.04	237.90	749.88	0.00	311.58	173.80	3,294	4.25	–	7.58	80
47	Menzel Chaker	Tarek Hammami	2,180.00	5.00	2,120.60	176.90	1345.55	0.00	89.14	546.10	6,708	9.28	–	7.27	90
48	Henchra	F. Hmed Mlawah	518.96	138.36	1,675.04	231.80	505.00	7.68	144.88	454.44	3,676	4.56	22.10	7.27	94
49	Henchra	F.Med Adwani	345.96	88.92	2,145.48	158.60	278.16	0.00	150.04	709.68	3,877	3.52	22.40	7.07	80
50	Henchra	F.Jarbouti	335.60	76.00	1,772.64	164.70	272.64	0.00	121.08	560.68	3,303	3.73	22.20	7.14	120
51	Henchra	F.Merkéz kammoun	432.68	151.16	1,713.00	219.60	376.92	0.00	152.40	477.76	3,524	4.29	22.20	7.07	120
52	Bir Ali Ben Khalifa	Khlifa Gdarat	78.84	27.81	246.15	378.20	270.63	0.00	19.55	31.90	1,053	1.24	14.50	7.70	107
53	Bir Ali Ben Khalifa	Taher Rahal	176.86	28.26	880.40	311.10	435.18	0.00	48.76	113.44	1,994	2.64	21.30	7.49	70
54	Menzel Chaker	Med Masmoudi	239.20	58.80	1,395.60	372.10	759.00	0.00	79.88	123.00	3,028	3.82	20.70	7.60	137
55	Menzel Chaker	CFJR	300.36	10.80	360.73	274.50	200.50	12.00	73.08	139.40	1,371	1.91	21.70	7.82	124
56	Menzel Chaker	Hafedh Jarraya (Ksar Irrih)	3,788.50	10.00	1,757.80	128.10	1,886.00	41.30	470.00	771.00	8,853	12.09	21.60	7.31	180
57	Agareb	Mustapha Frikha N. 1	1,645.10	68.50	1,724.00	207.40	1,166.10	0.00	242.20	505.10	5,681	9.90	–	7.45	160
58	Djebeniana	Jamel laarif	1,250.70	144.15	1,599.65	183.00	766.30	0.00	198.80	508.05	4,828	5.92	23.00	7.30	125
59	Agareb	Khalil Emmouri	369.88	4.00	2,061.64	189.10	576.28	4.00	166.48	404.12	3,776	–	–	–	115
60	Skhira	Mohamed Ben Omor	479.00	87.20	2,020.60	250.10	334.44	23.60	153.92	682.52	4,031	4.49	22.70	7.30	63
61	Skhira	Hamaada	458.55	95.00	2,394.60	164.70	497.95	42.20	173.95	589.95	4,417	4.88	23.90	7.31	63
62	Skhira	Henchr Gara	228.36	93.44	1,967.56	170.80	191.48	12.72	137.04	592.68	3,394	3.59	23.00	7.27	60
63	Menzel Chaker	Fawzi Mseddi	1,053.32	0.00	872.52	176.90	682.56	19.88	96.56	234.40	3,136	–	–	–	247
64	Agareb	Forage Agareb	206.86	20.04	1,142.58	219.60	482.62	10.02	60.94	129.90	2,273	2.82	–	7.39	113
65	Bir Ali Ben Khalifa	F. Neila Eleuch (Debut de L'essai)	1,354.05	64.80	1,348.15	183.00	765.00	0.00	241.40	490.10	4,801	–	–	–	175
66	Bir Ali Ben Khalifa	F. Neila Eleuch (Fin de L'essai)	1,389.25	39.25	1,292.40	164.50	781.90	0.00	211.10	464.10	4,638	–	–	–	175
67	Bir Ali Ben Khalifa	Gargouri Anouar	790.92	4.00	666.56	219.60	591.56	43.36	83.92	150.16	2,550	–	–	–	–
68	Skhira	Mohamed Eddib	404.65	33.85	2,067.00	91.50	466.45	13.65	123.40	559.90	3,760	4.51	–	7.52	55
69	Skhira	Noamen Mhadbi	278.90	46.95	1,939.60	122.00	246.55	17.60	133.50	572.55	3,358	3.87	–	7.33	55
70	Skhira	Mbarek Neyli	673.30	39.00	2,392.80	158.60	649.65	28.35	168.95	577.45	4,688	5.37	–	7.70	60
71	Skhira	Omor Ben Salah	479.60	33.15	1,979.35	97.60	375.60	12.80	136.85	629.65	3,745	4.45	–	7.52	68
72	Skhira	Mongi Ben chibéni	393.15	10.00	2,105.95	109.80	396.05	17.05	119.45	578.60	3,730	4.30	–	7.75	68
73	Skhira	Mohamed Khiri	1,140.90	22.85	2,403.00	122.00	861.25	32.50	133.40	571.25	5,260	6.33	–	7.16	70
74	Skhira	Hédi Démi	440.50	35.60	2,078.20	97.60	353.95	16.10	143.30	597.90	3,763	4.43	–	7.56	72
75	Skhira	Mohsen Mayeh	438.30	12.55	2,062.35	128.10	374.40	23.15	111.30	611.05	3,767	4.26	–	7.57	75
76	Skhira	Khalifa Lazzez	709.30	19.10	2,312.10	128.10	702.40	17.45	141.85	582.35	4,613	5.78	–	7.47	80
77	Skhira	Ferjani Yamina	2,298.40	4.40	2,994.20	146.40	1,460.10	28.00	336.80	684.50	7,953	10.40	–	7.80	80
78	–	Moncef Gdoura	791.60	0.00	1,531.65	183.00	893.35	26.65	99.05	256.35	3,782	4.96	–	7.58	–
79	Sfax km 10	Mahdi Trabelsi	415.95	19.20	1,256.05	250.10	570.00	23.65	104.80	222.05	2,862	3.52	22.50	7.34	–
80	Menzel Chaker-Sidi Litayem	Fawzi Mseddi 2	1,514.30	0.00	1,261.10	158.60	806.40	27.35	163.45	398.40	4,330	6.49	25.80	7.21	247
81	Bir Ali Ben Khalifa	Chaal 7 Bis	69.06	11.45	233.84	347.70	189.37	3.65	19.69	37.65	912	1.68	–	7.51	90
82	Menzel Chaker	Fraj Ghribi	748.75	217.30	2,246.15	122.00	583.90	18.55	191.65	643.65	4,772	5.52	22.10	8.13	–
83	Menzel Chaker	Rajab el Hedi	547.85	67.35	1,372.70	231.80	785.25	19.85	96.95	178.85	3,301	4.11	23.90	6.82	150
84	Menzel Chaker	Sofiene Kallel	1,720.45	56.00	1,480.75	128.10	921.40	28.60	247.85	420.60	5,004	4.18	24.60	6.76	180
85	Menzel Chaker	Med Chabchoub 3	1,024.50	105.60	2,444.55	134.20	840.00	18.20	241.80	571.15	5,380	6.71	22.60	6.96	110

Table 1 (continued)

Site/sample No. (Fig. 4)	Sample location	Sample name	Cl (mg/L)	NO ₃ (mg/L)	SO ₄ (mg/L)	HCO ₃ (mg/L)	Na (mg/L)	K (mg/L)	Mg (mg/L)	Ca (mg/L)	TDS (mg/L)	EC (µS/cm)	T (°C)	pH	Borehole depth (m)
86	Bir Ali Ben Khalifa	Mouldi bilayedti ben ali	1,208.70	68.10	1,807.55	115.90	792.30	13.50	220.70	444.00	4,671	6.36	23.80	6.84	112
87	Ltaifa	Hamaa Belhaj Itaief	74.67	49.37	221.47	237.90	169.28	9.01	21.42	52.41	836	1.01	23.50	6.93	65
88	Ltaifa	Abouda Zribi	100.38	33.18	460.35	213.50	259.62	8.58	20.32	57.90	1,154	1.74	22.80	6.97	92
89	Ltaifa	Forage Taoula (Zribi)	163.62	40.19	468.84	201.30	254.66	8.06	28.39	74.28	1,239	1.91	22.80	6.99	60
90	Ltaifa	Abdelkader Belhaj Itaief	106.70	27.64	723.90	256.20	390.38	6.80	29.48	54.50	1,596	2.71	24.60	6.90	110
91	Ltaifa	Mohamed Ben Nasr	109.44	34.93	441.83	280.60	255.19	3.82	22.73	56.40	1,205	1.84	24.50	7.04	80
92	Ltaifa	Noemen Belhaj Itaief	23.37	29.22	67.52	207.40	75.81	1.40	16.51	30.49	452	0.72	23.20	7.35	96
93	Bir Ali Ben Khalifa	Salah Oued Rkham	587.65	33.50	1,737.20	122.00	622.90	13.05	156.60	319.60	3,593	4.74	24.40	6.96	110
94	Menzel Chaker	Belgacem Fannassi	794.40	4.00	1,060.48	209.10	685.28	0.00	131.04	219.68	3,104	4.44	24.00	7.54	450
95	Bouthadi-Menzel Chaker	Belgacem Mabrouki	924.80	23.20	1,149.00	152.50	693.60	25.60	135.45	245.70	3,350	4.69	–	6.93	430
96	Bouthadi-Menzel Chaker	Belgacem Mabrouki N°2	689.55	20.25	1,187.20	183.00	695.60	36.50	120.80	211.15	3,144	3.90	–	7.37	360
97	Bouthadi-Menzel Chaker	Belgacem Mabrouki No. 3	811.30	14.65	1,021.90	183.00	628.45	13.95	109.20	197.70	2,980	4.37	–	7.56	508
98	Djebeniana-Nweyil	Mounir El ighali	878.85	160.65	1,096.15	152.50	338.15	17.20	96.20	586.05	3,326	4.52	22.00	6.74	80
99	Djebeniana-Iberma	Naceur Ben Ali	1,289.90	35.65	1,713.70	122.00	611.20	13.30	224.70	577.05	4,588	5.98	22.6	6.75	100
100	Djebeniana-Msetria	Salem Baccouche	1,164.85	23.25	1,279.70	176.90	611.10	15.00	148.05	456.00	3,875	5.89	22.9	6.68	65
101	Djebeniana-Iberma	Hakim Bouzayene	1,392.60	53.85	1,735.35	152.50	681.05	25.30	215.70	603.45	4,860	6.75	23.2	6.83	100
102	Djebeniana-Hzag	Forage Hzag	1,021.65	41.90	1,896.05	115.90	601.35	11.85	223.30	538.45	4,450	5.23	21.9	6.78	70
103	Djebeniana-Mnasria	Naceur Thkir	854.60	43.95	1,598.75	122.00	496.70	9.20	190.05	458.70	3,774	4.96	23.00	6.62	112
104	Djebeniana-Mnasria	Med Mansouri	455.00	49.20	1,462.85	122.00	285.45	12.15	135.90	462.50	2,985	3.89	23.4	6.68	94
105	Amra-Keitra	Med Maouei	780.05	38.05	2,553.40	152.50	804.45	15.20	191.15	554.55	5,089	6.82	22.7	6.84	80
106	Mahres	Sté El Itha (Abdelaziz Makhloufi)	1,096.30	0.00	1,107.40	183.00	779.90	23.00	124.75	273.75	3,588	5.27	–	7.68	80
107	Route Menzel Chaker	Forage Rami	1,000.45	29.05	2,374.75	231.80	761.35	21.60	200.55	609.80	5,229	–	–	–	–
108	Bir Ali Ben Khalifa	Sadok Rwag (AGIL)	2,040.00	18.00	2,991.60	140.30	1,443.50	28.80	319.90	624.60	7,607	9.68	26.20	7.36	160
109	Ltaifa	Bechir Haj Itaief	133.88	13.92	431.64	286.70	242.30	3.46	31.12	96.82	1,240	1.99	22.60	7.68	100
110	Bouladhieb-Agareb	Amor Mezghanni	1,349.80	3.85	2,001.65	134.20	976.25	21.15	181.30	376.75	5,045	6.88	24.00	7.41	100
111	Bouladhieb-Agareb	Amor Mezghanni (Societe el Baraka)	668.00	0.00	2,989.65	213.50	1,246.20	16.55	202.45	393.75	5,730	8.23	23.80	7.60	140
112	Agareb	Mustapha Frikha 2	1,134.55	0.00	819.70	195.20	683.95	21.90	105.70	229.80	3,191	5.08	24.20	7.76	242
113	Zeliana-Agareb	Jamil Triki	815.00	7.90	2,128.25	140.30	819.10	28.55	173.90	414.00	4,527	5.15	23.60	7.56	115
114	Zeliana-Agareb	Abdel Majid Ben Mansour	225.40	45.55	2,513.45	146.40	448.75	22.75	178.35	564.25	4,145	4.39	18.90	7.42	65
115	Skhira	Fakhreddine Ben kridis	913.90	23.75	2,263.50	140.30	858.00	26.40	147.35	481.95	4,855	6.23	24.30	7.83	124
116	Skhira	Lazhar Bali	484.40	5.70	2,719.75	54.90	811.65	23.75	123.75	521.45	4,745	5.46	21.20	7.74	120

intermediate aquifer range from 14.5 to 26.2 °C. The pH of these groundwater samples ranges from 5.85 to 8.13. The electrical conductivity (EC) value of the groundwater samples varies from 640 to 13,320 $\mu\text{S}/\text{cm}$. The salinity measurements show a total dissolved solids (TDS) content within the range of 451–10,106 mg/L, implying that the high salinity values are chiefly governed by the high concentrations of sodium, calcium and sulfate, followed by chloride, which are the dominant constituents in the water samples, leading to the dominance of the Ca-Na-SO₄ and Ca-Na-Cl-SO₄ water types.

The hydrochemical facies of the groundwater were studied by plotting the concentrations of the major cations and anions as a Piper trilinear diagram (Fig. 5). Based on the dominance of major cationic and anionic species, five hydrochemical facies have been identified in the study area (Table 2): (1) Ca-Na-SO₄ is the predominant water type (~ 51% of samples), with a relative enrichment of Na versus Ca in most samples; followed by (2) a mixed Ca-Na-Cl-SO₄ type corresponding to 31% of the samples; (3) Na-HCO₃-SO₄ type is present in 9% of the water samples; (4) Na-Cl-SO₄ and (5) Ca-Na-HCO₃ as minor water facies account for 7 and 3% of the groundwater samples, respectively (Fig. 6). These minor water types are observed in the recharge area (western part), where the groundwater salinity values are all less than 1,500 mg/L, likely originating from the dissolution of carbonates, or influenced by rain water infiltration or dissolution of the atmospheric CO₂. The predominant Ca-Na-SO₄ water type reflects that the aquifer formations are dominated by evaporate minerals such as halite, gypsum and anhydrite. Additionally, sulfate-rich rocks are commonly associated with dolomite, calcite and clays. In contrast, the Ca-Na-Cl-SO₄ water type is especially dominant in the northern part of the Sfax basin, particularly in Menzel Chaker and Djebeniana regions (see Fig. 3) where groundwater

salinity is high. This higher level of salinity could be related to Na-Cl dissolution or to cation exchange process for the coastal groundwater samples particularly in Djebeniana (Nos. 100 and 102) where borehole depths are 65 and 70 m respectively (Table 2). This pattern may suggest descendant water migration from the shallow aquifer to the intermediate aquifer. This migration of shallow water—where cation exchange through the clayey layers, separating the shallow and the intermediate aquifer, is occurring—leads to diverse typical facies such as Na-Cl-SO₄ and Ca-Na-SO₄ facies. The different hydrochemical facies mainly reflect the presence of high concentrations of Na⁺ and Ca²⁺ for the cations and Cl⁻ and SO₄²⁻ for the anions, representing the main contributors to the groundwater chemistry due to the dissolution effect. Generally, the hydrochemical composition of fresh groundwater in the Sfax aquifers is typically dominated by Ca²⁺, Na⁺ and HCO₃⁻ ions, as observed in certain samples (Nos. 17, 18, 20, 32, 52, 81, 87, and 92), and are located in the western part of the basin (Bir Ali ben Khalifa region). This area constitutes the recharge area and presents high piezometric levels, which explains the low salinities of the samples due to rapid infiltration of the water. The rapid infiltration is ensured by the wadi Chaal, located in the eastern part of Bir Ali Ben Khalifa region, and explains the low mineralization due to the limited water–rock interaction. The depletion in Ca²⁺ content relative to SO₄²⁻ concentration could be related to several processes: (1) cation exchange reactions in which Ca²⁺ ions are adsorbed on clay minerals with simultaneous release of Na⁺ ions, which may justify the excess of Na⁺ contents, (2) dissolution of thenardite (Na₂SO₄) and/or of mirabilite (Na₂SO₄ 10H₂O), characteristic of confined evaporitic zone. If Na⁺ ions are derived from dissolution of evaporative minerals, they should balance Cl ion content. The cation exchange could be confirmed through the plot of (Na + K) – Cl versus [(Ca + Mg) – (SO₄ + HCO₃)] (Fig. 7), which reveals a release of Na⁺ ions with respect to a decrease of Ca²⁺ ions. The sampled groundwaters that are located in the downstream part, represent an excess of Na⁺ with respect to Cl⁻. This excess could be explained by cation exchange reactions (type I) which absorb Ca²⁺ on the clay fraction as Na⁺ is released, while significant deficit of Na⁺ is observed in the sampled groundwaters situated in the upstream (the left side of Fig. 7). This might stem from the second type (type II) of cation exchange where Na⁺ ions are removed from the solution and are replaced by Ca²⁺ ions. The calculated saturation indices with respect to various mineral phases (i.e., calcite, dolomite, gypsum and halite) of the groundwater samples are shown in Table 2. The positive and negative SI values represent the thermodynamic potential for precipitation and dissolution, respectively. Dissolution of evaporites is also confirmed by the saturation indices (Table 2). They show that almost all samples are undersaturated with respect to halite. The sulfate minerals of thenardite and/or mirabilite are characteristic of an arid area and are formed in a confined evaporitic depressions, which is in good agreement with the studied area. On the other side, the saturation indices show that almost all samples are

Hydrochemical facies

- 1: Ca-Na-SO₄
- 2: Ca-Na-Cl-SO₄
- 3: Na-HCO₃-SO₄
- 4: Na-Cl-SO₄
- 5: Ca-Na-HCO₃

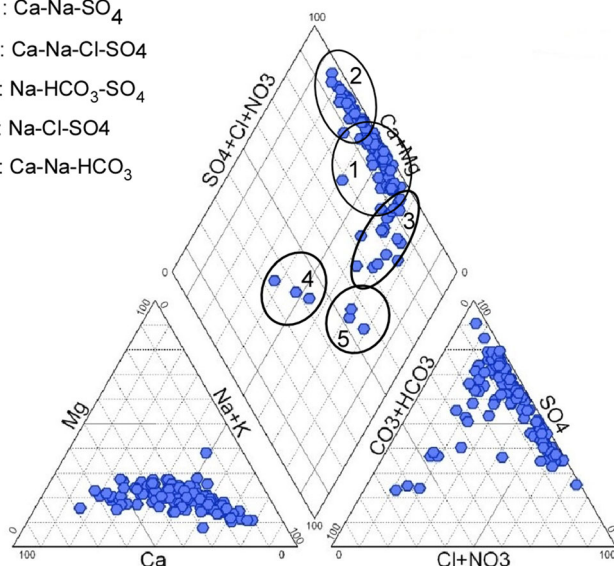


Fig. 5 Piper diagram of the analyzed groundwater

Table 2 Water classification groups, saturation indices (SI) values of carbonate and evaporates minerals and some ionic ratios for groundwater samples in the study area

Site/sample No.	Water type	SI Anhydrite	SI Aragonite	SI Calcite	SI Dolomite	SI Gypsum	SI Halite	SI Thenardite	SI Mirabilite	Na/Cl	SO ₄ /Cl	HCO ₃ /Cl	Ca/Na	Ca/SO ₄	Mg/Ca
1	Na-Cl-SO ₄	-0.29	-0.09	0.05	-0.19	-0.08	-3.90	-4.53	-3.61	0.82	0.55	0.03	0.42	0.63	1.32
2	Ca-Na-SO ₄	-0.24	-0.09	0.06	-0.59	-0.02	-5.03	-5.50	-4.57	1.03	1.94	0.10	1.29	0.69	0.53
3	Ca-Na-SO ₄	-0.60	-0.08	0.07	-0.51	-0.38	-6.06	-6.26	-5.33	2.53	5.89	0.92	1.34	0.58	0.62
4	Ca-Na-SO ₄	-0.29	-0.30	-0.16	-1.01	-0.07	-5.63	-5.97	-5.04	1.38	4.20	0.17	1.90	0.62	0.55
5	Ca-Na-Cl-SO ₄	-0.20	-0.15	-0.01	-0.55	0.02	-4.34	-4.88	-3.95	0.87	0.96	0.03	0.70	0.65	0.79
6	Ca-Na-Cl-SO ₄	-0.48	-0.05	0.09	-0.40	-0.26	-4.63	-5.36	-4.44	0.84	0.74	0.08	0.80	0.74	0.68
7	Ca-Na-SO ₄	-0.96	-0.35	-0.20	-0.81	-0.74	-5.34	-5.57	-4.64	2.43	2.26	0.48	0.26	0.28	1.06
8	Ca-Na-SO ₄	-0.35	-0.25	-0.11	-0.73	-0.14	-5.11	-5.20	-4.27	2.03	3.37	0.17	0.66	0.40	0.84
9	Ca-Na-SO ₄	-0.29	-0.22	-0.08	-0.66	-0.07	-4.96	-5.02	-4.10	2.05	3.12	0.14	0.66	0.41	0.83
10	Ca-Na-SO ₄	-0.36	-0.24	-0.09	-0.72	-0.14	-5.11	-5.21	-4.28	2.02	3.27	0.18	0.66	0.41	0.81
11	Ca-Na-SO ₄	-0.29	-0.20	-0.06	-0.63	-0.08	-5.24	-5.26	-4.33	2.35	4.37	0.21	0.82	0.44	0.84
12	Na-Cl-SO ₄	-0.35	-0.35	-0.21	-0.71	-0.13	-3.89	-4.47	-3.56	0.88	0.55	0.02	0.34	0.55	1.34
13	Ca-Na-SO ₄	-0.37	-0.29	-0.14	-1.19	-0.15	-5.62	-6.26	-5.33	0.97	2.40	0.12	2.30	0.93	0.34
14	Ca-Na-SO ₄	-0.26	-0.18	-0.03	-1.13	-0.04	-5.91	-6.64	-5.70	0.75	3.21	0.16	4.54	1.06	0.23
15	Ca-Na-SO ₄	-0.42	-0.17	-0.02	-0.70	-0.20	-4.88	-5.35	-4.42	1.25	1.41	0.10	0.73	0.64	0.60
16	Ca-Na-SO ₄	-0.62	-0.28	-0.14	-0.90	-0.40	-5.04	-5.26	-4.33	1.98	2.02	0.20	0.40	0.39	0.65
17	Ca-Na-HCO ₃	-1.97	-0.43	-0.28	-1.20	-1.75	-7.17	-7.94	-7.01	5.19	2.58	6.32	0.68	1.37	0.61
18	Na-HCO ₃ -SO ₄	-1.79	-0.52	-0.38	-1.41	-1.57	-6.56	-6.94	-6.01	6.06	2.97	3.82	0.25	0.27	0.84
19	Ca-Na-SO ₄	-0.74	-0.46	-0.32	-1.15	-0.52	-5.17	-5.25	-4.32	2.51	2.72	0.25	0.29	0.27	0.84
20	Ca-Na-HCO ₃	-2.00	-0.39	-0.24	-1.16	-1.78	-7.51	-8.32	-7.38	5.96	3.31	9.46	1.08	1.94	0.55
21	Ca-Na-SO ₄	-0.97	-0.38	-0.24	-1.04	-0.75	-5.61	-5.74	-4.81	3.18	3.21	0.67	0.31	0.31	0.75
22	Ca-Na-SO ₄	-0.69	-0.42	-0.27	-1.06	-0.47	-5.15	-5.35	-4.42	2.13	2.27	0.20	0.37	0.35	0.83
23	Ca-Na-SO ₄	-0.55	-0.26	-0.11	-0.80	-0.33	-5.17	-5.47	-4.54	1.79	2.15	0.19	0.61	0.51	0.72
24	Ca-Na-SO ₄	-0.61	-0.42	-0.27	-1.09	-0.39	-5.28	-5.27	-4.34	2.87	3.66	0.26	0.40	0.31	0.79
25	Ca-Na-SO ₄	-0.26	-0.24	-0.10	-0.98	-0.04	-4.93	-4.93	-4.46	1.10	1.70	0.07	1.07	0.69	0.44
26	Ca-Na-SO ₄	-0.64	-0.27	-0.13	-0.91	-0.42	-5.35	-5.42	-4.49	2.78	3.27	0.37	0.45	0.38	0.61
27	Ca-Na-SO ₄	-0.35	-0.17	-0.03	-0.71	-0.13	-4.75	-5.14	-4.21	1.34	1.48	0.09	0.67	0.61	0.59
28	Ca-Na-SO ₄	-0.23	-0.25	-0.11	-0.95	-0.01	-5.05	-5.24	-4.31	1.60	2.92	0.11	0.91	0.50	0.51
29	Ca-Na-Cl-SO ₄	-0.19	-0.25	-0.11	-0.71	0.02	-4.30	-4.87	-3.95	0.84	0.88	0.02	0.74	0.70	0.84
30	Ca-Na-SO ₄	-0.42	-0.39	-0.24	-1.00	-0.20	-5.16	-5.05	-4.12	3.04	4.39	0.20	0.48	0.33	0.84
31	Ca-Na-SO ₄	-0.99	-0.30	-0.16	-0.79	-0.77	-5.57	-5.67	-4.74	3.25	3.28	0.86	0.27	0.27	0.92
32	Na-HCO ₃ -SO ₄	-1.30	-0.37	-0.22	-1.02	-1.08	-6.05	-6.15	-5.22	5.15	3.99	2.05	0.25	0.33	0.72
33	Ca-Na-Cl-SO ₄	-0.33	-0.03	0.12	-0.32	-0.11	-4.54	-5.39	-4.47	0.67	0.68	0.05	1.07	1.06	0.74
34	Ca-Na-SO ₄	-0.97	-0.32	-0.17	-0.92	-0.75	-5.55	-5.87	-4.94	2.47	2.19	0.52	0.38	0.43	0.72
35	Ca-Na-SO ₄	-0.24	-0.28	-0.13	-0.92	-0.02	-5.36	-5.46	-4.53	2.03	4.42	0.16	1.16	0.54	0.61
36	Ca-Na-SO ₄	-0.06	-0.01	0.14	-0.41	0.16	-6.00	-5.64	-4.71	4.93	18.76	0.80	2.13	0.56	0.56
37	Ca-Na-SO ₄	-0.69	-0.32	-0.18	-1.12	-0.47	-5.64	-4.83	-4.83	3.06	3.76	0.44	0.60	0.49	0.47
38	Ca-Na-Cl-SO ₄	-0.10	-0.09	0.06	-0.60	0.12	-4.29	-4.69	-3.77	1.13	1.12	0.04	0.72	0.73	0.52
39	Ca-Na-SO ₄	-0.27	-0.08	0.06	-0.57	-0.05	-4.93	-5.01	-4.09	2.18	2.82	0.17	0.66	0.51	0.54
40	Ca-Na-SO ₄	-0.42	-0.25	-0.10	-0.70	-0.20	-4.84	-4.95	-4.02	2.02	2.36	0.14	0.43	0.37	0.87
41	Ca-Na-Cl-SO ₄	-0.69	-0.23	-0.09	-0.77	-0.47	-4.67	-4.56	-4.56	0.83	0.56	0.07	0.52	0.76	0.68
42	Ca-Na-Cl-SO ₄	-0.65	-0.17	-0.03	-0.83	-0.43	-4.81	-5.61	-4.68	0.97	0.65	0.08	0.66	0.99	0.45
43	Ca-Na-SO ₄	-0.45	-0.30	-0.16	-0.88	-0.23	-5.38	-5.42	-4.40	2.47	4.26	0.27	0.67	0.38	0.74
44	Ca-Na-SO ₄	-0.73	-0.49	-0.35	-1.29	-0.51	-5.84	-5.94	-5.01	3.07	4.82	0.42	0.67	0.42	0.70
45	Ca-Na-SO ₄	-1.13	-0.60	-0.46	-1.13	-0.92	-5.81	-5.65	-4.72	6.00	5.28	1.03	0.19	0.22	0.81
46	Na-Cl-SO ₄	-0.91	-0.38	-0.24	-0.43	-0.69	-5.09	-5.41	-4.49	2.16	1.90	0.26	0.27	0.30	2.96
47	Na-Cl-SO ₄	-0.34	-0.11	0.03	-0.93	-0.12	-4.79	-4.27	-3.86	0.95	0.72	0.05	0.47	0.62	0.27
48	Na-Ca-Cl-SO ₄	-0.41	0.00	0.14	-0.42	-0.19	-5.28	-5.65	-4.72	1.50	2.38	0.26	1.03	0.65	0.53
49	Ca-Na-SO ₄	-0.17	-0.01	0.14	-0.61	0.05	-5.72	-6.11	-5.18	1.24	4.58	0.27	2.93	0.79	0.35
50	Ca-Na-SO ₄	-0.29	-0.06	0.09	-0.71	-0.07	-5.73	-6.16	-5.23	1.25	3.90	0.29	2.36	0.76	0.36

Table 2 (continued)

Site/sample No.	Water type	SI Anhydrite	SI Aragonite	SI Calcite	SI Dolomite	SI Gypsum	SI Halite	SI Thenardite	SI Mirabilite	Na/Cl	SO ₄ /Cl	HCO ₃ /Cl	Ca/Na	Ca/SO ₄	Mg/Ca
51	Ca-Na-SO ₄	-0.38	0.00	0.14	-0.43	-0.16	-5.48	-5.90	-4.97	1.34	2.92	0.29	1.45	0.67	0.53
52	Na-HCO ₃ -SO ₄	-1.91	-0.66	-0.52	-1.46	-1.69	-6.28	-6.67	-5.73	5.29	2.30	2.79	0.14	0.31	1.01
53	Ca-Na-SO ₄	-1.05	-0.36	-0.22	-1.01	-0.83	-5.77	-5.86	-4.93	3.79	3.67	1.02	0.30	0.31	0.71
54	Ca-Na-SO ₄	-0.95	-0.33	-0.19	-0.79	-0.73	-5.42	-5.26	-4.33	4.89	4.31	0.90	0.19	0.21	1.07
55	Ca-Na-Cl-SO ₄	-1.26	-0.22	-0.08	-0.64	-1.04	-5.85	-6.91	-5.98	1.03	0.89	0.53	0.80	0.93	0.86
56	Ca-Na-Cl-SO ₄	-0.42	-0.13	0.01	-0.38	-0.20	-3.91	-4.76	-3.84	0.77	0.34	0.02	0.47	1.05	1.01
57	Ca-Na-Cl-SO ₄	-0.46	-0.04	0.10	-0.33	-0.24	-4.44	-5.03	-4.10	1.09	0.77	0.07	0.50	0.70	0.79
58	Ca-Na-Cl-SO ₄	-0.44	-0.07	0.07	-0.47	-0.22	-4.73	-5.38	-4.45	0.94	0.94	0.09	0.76	0.76	0.65
59	Ca-Na-SO ₄	-0.40	-0.17	-0.03	-0.66	-0.18	-5.37	-5.45	-4.52	2.40	4.11	0.30	0.80	0.47	0.68
60	Ca-Na-SO ₄	-0.21	0.18	0.32	-0.22	0.01	-5.50	-5.98	-5.05	1.08	3.11	0.30	2.34	0.81	0.37
61	Ca-Na-SO ₄	-0.22	-0.09	0.05	-0.65	0.00	-5.35	-5.56	-4.63	1.67	3.85	0.21	1.36	0.59	0.49
62	Ca-Na-SO ₄	-0.24	-0.03	0.11	-0.63	-0.02	-6.05	-6.43	-5.50	1.29	6.36	0.43	3.55	0.72	0.38
63	Ca-Na-Cl-SO ₄	-0.86	-0.32	-0.18	-0.95	-0.64	-4.83	-5.61	-4.68	1.00	0.61	0.10	0.39	0.64	0.68
64	Ca-Na-SO ₄	-0.94	-0.49	-0.35	-1.24	-0.72	-5.67	-5.69	-4.76	3.60	4.08	0.62	0.31	0.27	0.77
65	Ca-Na-Cl-SO ₄	-0.53	-0.07	0.08	-0.36	-0.31	-4.70	-5.47	-4.54	0.87	0.73	0.08	0.73	0.87	0.81
66	Ca-Na-Cl-SO ₄	-0.55	-0.13	0.01	-0.52	-0.33	-4.67	-5.45	-4.53	0.87	0.69	0.07	0.68	0.86	0.75
67	Ca-Na-Cl-SO ₄	-1.10	-0.38	-0.24	-0.93	-0.88	-5.00	-5.79	-4.86	1.15	0.62	0.16	0.29	0.54	0.92
68	Ca-Na-SO ₄	-0.26	-0.34	-0.20	-1.27	-0.04	-5.42	-5.64	-4.71	1.78	3.77	0.13	1.38	0.65	0.36
69	Ca-Na-SO ₄	-0.24	-0.19	-0.04	-0.94	-0.04	-5.86	-6.21	-5.28	1.36	5.13	0.25	2.66	0.71	0.38
70	Ca-Na-SO ₄	-0.24	-0.12	0.02	-0.71	-0.02	-5.07	-5.33	-4.41	1.49	2.62	0.14	1.02	0.58	0.48
71	Ca-Na-SO ₄	-0.24	-0.25	-0.11	-1.10	-0.02	-5.44	-5.87	-4.94	1.21	3.05	0.12	1.92	0.76	0.36
72	Ca-Na-Cl-SO ₄	-0.25	-0.25	-0.11	-1.12	-0.02	-5.51	-5.77	-4.84	1.55	3.95	0.16	1.68	0.66	0.34
73	Ca-Na-SO ₄	-0.24	-0.28	-0.14	-1.12	-0.02	-5.51	-5.77	-4.71	1.16	1.55	0.06	0.76	0.57	0.39
74	Ca-Na-SO ₄	-0.24	-0.16	-0.01	-0.96	-0.04	-5.49	-5.84	-4.96	1.24	3.48	0.13	1.94	0.69	0.40
75	Ca-Na-SO ₄	-0.23	-0.21	-0.06	-1.12	-0.02	-5.02	-5.28	-4.35	1.53	2.41	0.10	0.95	0.60	0.40
76	Ca-Na-SO ₄	-0.24	-0.21	-0.01	-0.96	-0.02	-5.02	-5.28	-4.35	1.53	2.41	0.10	0.95	0.60	0.40
77	Ca-Na-Cl-SO ₄	-0.21	-0.15	-0.01	-0.54	0.00	-4.23	-4.67	-3.75	0.98	0.96	0.04	0.54	0.55	0.81
78	Ca-Na-Cl-SO ₄	-0.66	-0.34	-0.20	-1.03	-0.44	-4.85	-5.16	-4.23	1.74	1.43	0.13	0.33	0.40	0.64
79	Ca-Na-SO ₄	-0.74	-0.23	-0.08	-0.71	-0.52	-5.30	-5.58	-4.65	2.11	2.23	0.35	0.45	0.42	0.78
80	Ca-Na-Cl-SO ₄	-0.60	-0.21	-0.06	-0.72	-0.38	-4.62	-5.41	-4.48	0.82	0.61	0.06	0.57	0.76	0.68
81	Na-HCO ₃ -SO ₄	-1.84	-0.61	-0.47	-1.42	-1.62	-6.49	-6.98	-6.05	4.23	2.50	2.92	1.26	0.39	0.86
82	Ca-Na-SO ₄	-0.23	-0.18	-0.04	-0.82	-0.01	-5.07	-5.47	-4.55	1.20	2.21	0.09	1.26	0.69	0.49
83	Na-Cl-SO ₄	-0.82	-0.38	-0.23	-0.95	-0.60	-5.05	-5.28	-4.35	2.21	1.85	0.25	0.26	0.31	0.89
84	Na-Cl-SO ₄	-0.57	-0.31	-0.16	-0.76	-0.35	-4.52	-5.27	-4.35	0.83	0.64	0.04	0.52	0.68	0.97
85	Ca-Na-Cl-SO ₄	-0.27	-0.21	-0.07	-0.73	-0.06	-4.79	-5.14	-4.22	1.26	1.76	0.08	0.78	0.56	0.70
86	Ca-Na-Cl-SO ₄	-0.45	-0.34	-0.19	-0.90	-0.23	-4.73	-5.29	-4.37	1.01	1.10	0.06	0.64	0.59	0.82
87	Na-HCO ₃ -SO ₄	-1.71	-0.62	-0.48	-1.55	-1.49	-6.50	-7.11	-6.18	3.50	2.19	1.85	0.36	0.57	0.67
88	Na-HCO ₃ -SO ₄	-1.45	-0.71	-0.56	-1.79	-1.23	-6.21	-6.47	-5.53	3.99	3.38	1.24	0.26	0.30	0.58
89	Na-HCO ₃ -SO ₄	-1.36	-0.63	-0.49	-1.36	-1.14	-6.01	-6.50	-5.57	2.40	2.11	0.71	0.33	0.38	0.63
90	Na-HCO ₃ -SO ₄	-1.38	-0.72	-0.58	-1.65	-1.16	-6.02	-5.97	-5.04	5.64	5.01	1.39	0.16	0.18	0.89
91	Na-HCO ₃ -SO ₄	-1.48	-0.60	-0.45	-1.52	-1.26	-6.18	-6.50	-5.57	3.60	2.98	1.49	0.25	0.31	0.66
92	Ca-Na-HCO ₃	-2.32	-0.82	-0.67	-1.82	-2.10	-7.33	-8.24	-7.30	5.00	2.13	5.16	0.46	1.08	0.89
93	Ca-Na-SO ₄	-0.54	-0.43	-0.29	-1.11	-0.32	-5.13	-5.44	-4.60	1.63	2.18	0.12	0.59	0.44	0.81
94	Ca-Na-Cl-SO ₄	-0.83	-0.30	-0.15	-0.74	-0.61	-4.95	-5.53	-4.60	1.33	0.99	0.15	0.37	0.50	0.98
95	Ca-Na-Cl-SO ₄	-0.77	-0.40	-0.25	-0.98	-0.55	-4.88	-5.50	-4.57	1.16	0.92	0.10	0.41	0.51	0.91
96	Ca-Na-Cl-SO ₄	-0.80	-0.38	-0.24	-0.94	-0.58	-5.00	-5.46	-4.53	1.56	1.27	0.15	0.35	0.43	0.94
97	Na-Cl-SO ₄	-0.87	-0.39	-0.25	-0.97	-0.65	-4.97	-5.60	-4.67	1.19	0.93	0.13	0.36	0.46	0.91
98	Ca-Na-Cl-SO ₄	-0.45	-0.02	0.12	-0.75	-0.23	-5.22	-6.20	-5.27	0.59	0.92	0.10	1.99	1.28	0.27
99	Ca-Na-Cl-SO ₄	-0.37	-0.20	-0.05	-0.73	-0.15	-4.82	-5.56	-4.63	0.73	0.98	0.05	1.08	0.81	0.64
100	Ca-Na-Cl-SO ₄	-0.52	-0.09	0.05	-0.59	-0.30	-4.85	-5.63	-4.70	0.81	0.81	0.09	0.86	0.85	0.54

Table 2 (continued)

Site/sample No.	Water type	SI Anhydrite	SI Aragonite	SI Calcite	SI Dolomite	SI Gypsum	SI Halite	SI Thenardite	SI Mirabilite	Na/Cl	SO ₄ /Cl	HCO ₃ /Cl	Ca/Na	Ca/SO ₄	Mg/Ca
101	Ca-Na-Cl-SO ₄	-0.36	-0.09	0.06	-0.54	-0.14	-4.74	-5.47	-4.54	0.75	0.92	0.06	1.02	0.83	0.59
102	Ca-Na-Cl-SO ₄	-0.35	-0.26	-0.11	-0.82	-0.14	-4.92	-5.52	-4.59	0.91	1.37	0.07	1.03	0.68	0.68
103	Ca-Na-Cl-SO ₄	-0.44	-0.27	-0.13	-0.85	-0.22	-5.07	-5.71	-4.79	0.90	1.38	0.08	1.06	0.69	0.68
104	Ca-Na-SO ₄	-0.42	-0.24	-0.09	-0.93	-0.20	-5.57	-6.18	-5.25	0.97	2.37	0.16	1.86	0.76	0.48
105	Ca-Na-SO ₄	-0.25	-0.17	-0.03	-0.74	-0.23	-4.92	-5.14	-4.50	1.59	2.42	0.11	0.79	0.52	0.57
106	Ca-Na-Cl-SO ₄	-0.75	-0.28	-0.13	-0.82	-0.53	-4.76	-5.43	-4.50	1.10	0.75	0.10	0.40	0.59	0.75
107	Ca-Na-Cl-SO ₄	-0.25	0.06	0.20	-0.30	-0.03	-4.84	-5.23	-4.30	1.17	1.75	0.13	0.92	0.62	0.54
108	Ca-Na-Cl-SO ₄	-0.24	-0.21	-0.06	-0.63	-0.02	-4.28	-4.66	-3.74	1.09	1.08	0.04	0.50	0.50	0.84
109	Na-HCO ₃ -SO ₄	-1.29	-0.36	-0.21	-1.13	-1.07	-6.11	-6.59	-5.66	2.79	2.38	1.24	0.46	0.54	0.53
110	Ca-Na-Cl-SO ₄	-0.48	-0.36	-0.22	-0.97	-0.26	-4.60	-5.05	-4.13	1.12	1.09	0.06	0.44	0.45	0.79
111	Na-Cl-SO ₄	-0.36	-0.21	-0.07	-0.64	-0.14	-4.81	-4.69	-3.77	2.88	3.30	0.19	0.36	0.32	0.85
112	Ca-Na-Cl-SO ₄	-0.90	-0.29	-0.14	-0.83	-0.68	-4.79	-5.64	-4.71	0.93	0.53	0.10	0.39	0.67	0.76
113	Ca-Na-SO ₄	-0.41	-0.30	-0.16	-0.91	-0.19	-4.89	-5.16	-4.24	1.55	1.93	0.10	0.58	0.47	0.69
114	Ca-Na-SO ₄	-0.22	-0.17	-0.02	-0.77	0.00	-5.70	-5.61	-4.68	3.07	8.23	0.38	1.44	0.54	0.52
115	Ca-Na-SO ₄	-0.33	-0.25	-0.11	-0.95	-0.11	-4.82	-5.11	-4.18	1.45	1.83	0.09	0.64	0.51	0.50
116	Ca-Na-SO ₄	-0.23	-0.65	-0.51	-1.86	-0.01	-5.12	-5.07	-4.14	2.58	4.14	0.07	0.74	0.46	0.39

undersaturated with respect to Na₂SO₄ and/or of Na₂SO₄ 10H₂O minerals (SI < 0), indicating their dissolution (Table 2).

The results of geochemical modeling suggest that most of the well water samples from the intermediate aquifer are saturated to undersaturated with respect to calcite (Table 2). Figure 8a,b shows a comparison of calcite and dolomite saturation indexes of all water samples as a function of HCO₃ concentration. Calcite precipitation may occur systematically for all groundwater samples, which implies the limited contribution of carbonate minerals in the groundwater evolution; hence, the proportions of Ca and HCO₃ decrease. In fact, the values of SI for calcite are close to equilibrium (SI = 0), ranging from -0.67 to 0.32, and for dolomite show an undersaturation state. The saturation of the groundwater samples with respect to calcite and the undersaturation of groundwater samples with respect to dolomite may be explained by the incongruent dissolution of dolomite and gypsum with simultaneous precipitation of calcite, which provide evidence for the depletion in Ca²⁺ content relative to SO₄²⁻ concentration. The occurrence of dedolomitization reactions in the studied aquifer has a large potential for substantial modification of the C isotope signature of the DIC pool formed in the recharge area. The saturation of the groundwater samples with respect to calcite and dolomite is explained by the outgassing of CO₂, which in most hydrological systems is the primary process responsible for the supersaturation of the analyzed groundwaters with respect to carbonate mineral (Edmunds et al. 2003). The samples are undersaturated with respect to dolomite. About 28% of all groundwater are undersaturated with respect to dolomite with SI < -1, which is observed in water samples Nos. 4, 13, 14, 17, 18, 19, 20, 21, 22, 24, 32, 37, 44, 45, 52, 53 and 64, among others (Table 2), indicating probably the significance of dolomite dissolution in this system, thereby adding Ca²⁺, Mg²⁺, and HCO₃⁻ to the solution. They are attributed to different hydrochemical facies. Almost all of this entire water group (61%) belongs to the Ca-Na-SO₄ water type, with 24% indicating Na-HCO₃-SO₄ water type. All groundwater samples exhibit a state of equilibrium to undersaturation with respect to gypsum and anhydrite, which confirms the role of gypsum and/or anhydrite dissolution (Fig. 8c). In contrast, all the sampled waters are undersaturated with respect to halite (Fig. 8d), which implies that considerable dissolution causing strong mineralization along the groundwater flow paths may occur. The high dissolution rate for evaporate rocks allows waters close to saturation with respect to gypsum. This indicates that the groundwater has the capacity to dissolve gypsum and halite along the flow paths; hence, the concentrations of Ca²⁺, SO₄²⁻, Na⁺ and Cl⁻ in the solution increase (Stumm and Morgan 1996). In addition, the ionic composition may be caused by several factors, including water-rock interaction, ionic exchange, etc.; hence, it is necessary to use ionic ratios to identify the factors responsible for the hydrochemical composition of the

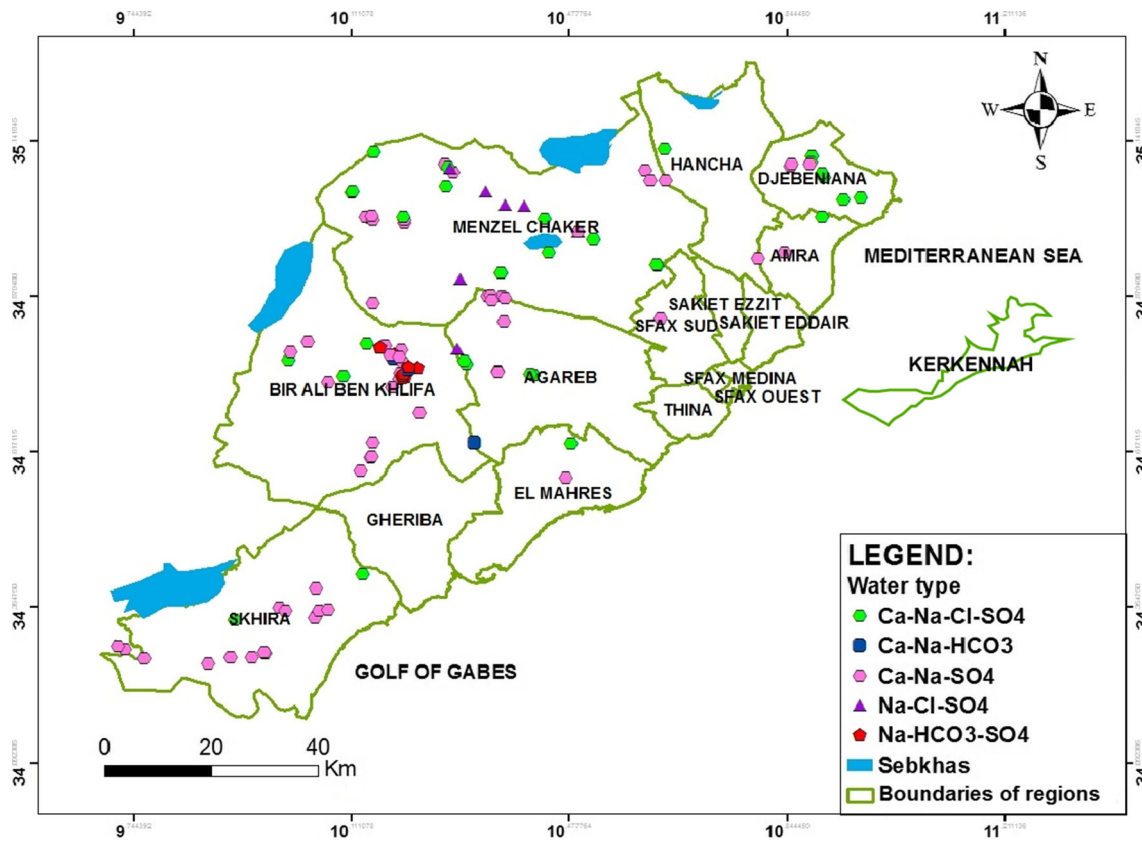


Fig. 6 Distribution of the water types

intermediate aquifer. Bivariate diagrams of ionic constituents have been developed (Na/Cl vs Cl , SO_4/Cl vs Cl , HCO_3/Cl vs Cl , and Ca/Na vs Cl) and are presented in Fig. 9. Generally, if halite dissolution is responsible for sodium and chloride, the Na/Cl molar ratio should be approximately one (Meybeck 1987). The Na/Cl ratios of water samples range from 0.67 to 6.06 (Table 2). The majority of the samples corresponding to 78% have molar ratios greater than or equal to one, which indicate that the increase in Na^+ ions could be linked to (1) ion exchange and/or (2) evaporate minerals dissolution as demonstrated previously; however, some water samples

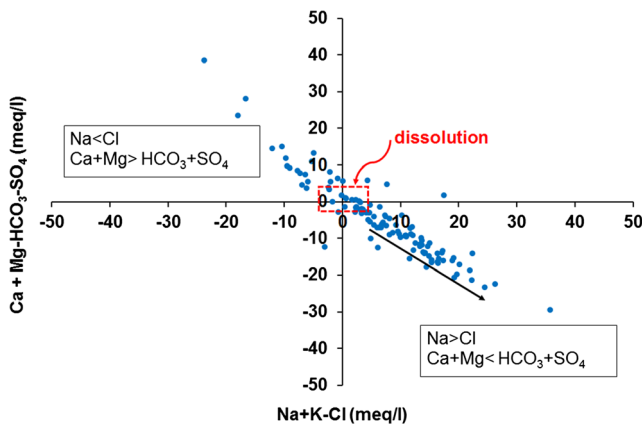


Fig. 7 Plot of $(\text{Ca} + \text{Mg}) - (\text{HCO}_3 + \text{SO}_4)$ vs. $\text{Na} + \text{K} - \text{Cl}$ in meq/L

(Nos. 1, 5, 6, 12, 14, 29, 33, 41, 56, 65 and 66, among others) mainly belong to the group of Ca-Na-Cl-SO_4 type, showing Na/Cl molar ratios less than 1. This indicates possible mixing with saline water, through a vertical leakage, likely originating from the shallow groundwater or from a deep saline adjacent aquifer level. This group of samples, which are enriched in Cl^- contents, features salinity values ranging from 3,135 to 10,106 mg/L. The plot of Na/Cl and SO_4/Cl ratios versus Cl^- concentrations suggests that these ratios increase with decreasing salinity and vary between water types (Fig. 9a,b). The HCO_3/Cl ratios provide a clear picture of the relative concentrations of chloride and bicarbonate; thus, this ratio can be a good indicator for salinization. The ratios of HCO_3/Cl , indicative of freshwater recharge, are high (> 1) in samples Nos. 17, 18, 20, 32, 45, 52, 53, 81, 87, 88, 90, 91, 92 and 109 located in the western part of the study area (recharge areas), where salinities are less than 2,000 mg/L; however, the majority of the groundwater samples belonging to the mixed Ca-Na-Cl-SO_4 type have lower HCO_3/Cl ratio values, indicating possible mixing with salt water. During the mixing process, the groundwater becomes enriched in Cl^- , which leads to a decrease in the value of the HCO_3/Cl ratio (Fig. 9c). This mixing process may be the result of the groundwater interaction between the aquifers (Ayadi et al. 2016), and further affects the amount and type of dissolved solids in the groundwater. In this case, the samples located in the northern part of

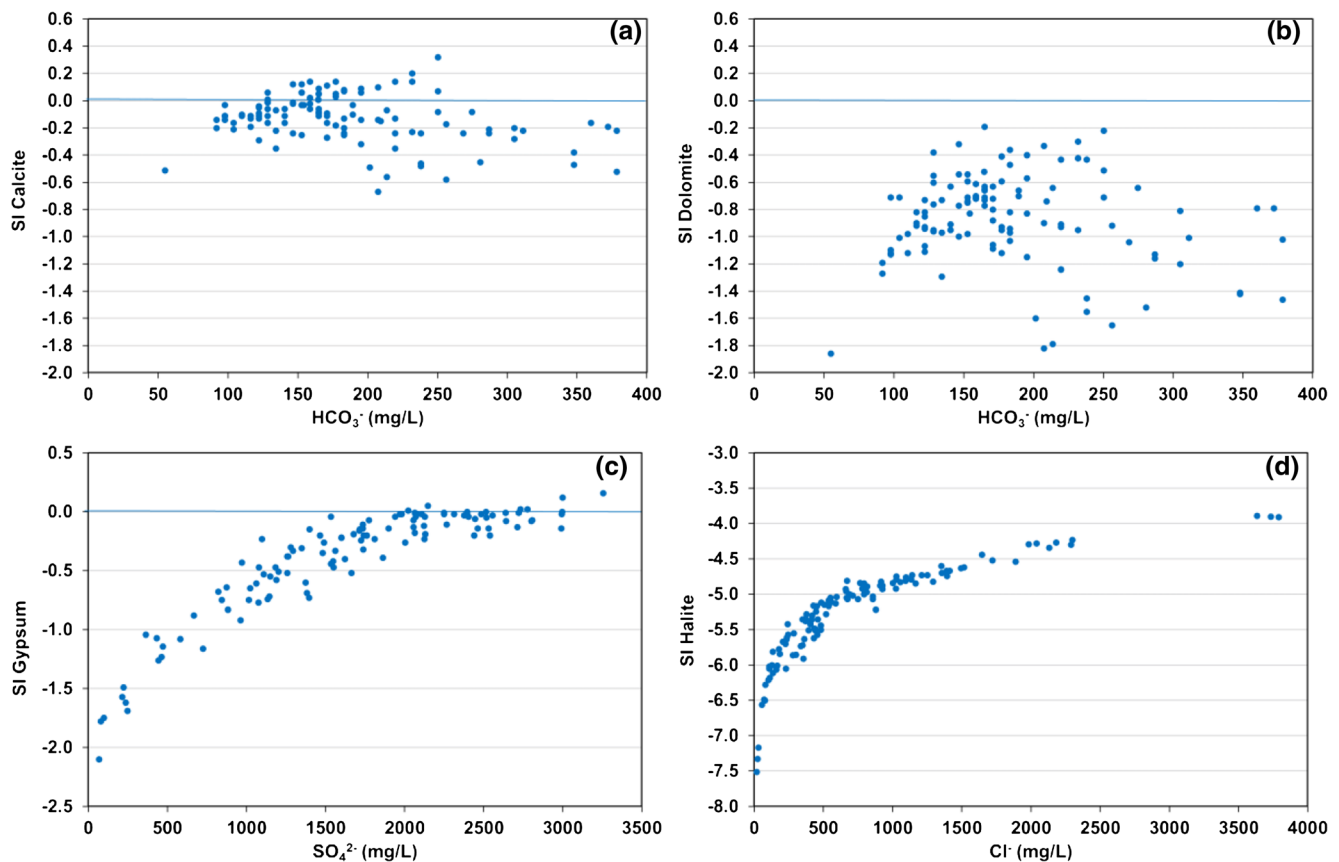


Fig. 8 a Calcite saturation index (SI) versus HCO_3^- ; b Dolomite saturation index versus HCO_3^- ; c Gypsum saturation index versus SO_4^{2-} ; d Halite saturation index versus Cl

Sfax, nearest to the sabkhas, have the highest total dissolved solids, which can reach 10,000 mg/L (sample No. 1), belonging to Na-Cl- SO_4 type. These water samples also show a large range of Ca/Na ratios (0.13–4.54). These ratios increase with reduced salinity and vary between water types. For the groundwater with high Ca/Na molar ratios, i.e., much greater than 1, the prevailing processes in the aquifer matrix are carbonate dissolution and/or depletion of Na (Fig. 9d).

Isotopic study

Stable isotope analysis of the groundwater

The isotopic composition ($\delta^{18}\text{O}$ and $\delta^2\text{H}$) and the calculated deuterium excess values of groundwater samples are presented in Table 3. The stable isotope composition of the groundwater samples from the intermediate aquifer varies within a wide range from -6.86 to -2.97 ‰ for $\delta^{18}\text{O}$ and from -44.2 to -22.4 ‰ for $\delta^2\text{H}$. For the isotopic characterization of the samples from the intermediate aquifer of Sfax, the isotope data of sampled waters were plotted in the binary diagram of $\delta^2\text{H}$ - $\delta^{18}\text{O}$ (Fig. 10). The Global Meteoric Water Line (GMWL; Craig 1961), and the local meteoric water line for Sfax (LMWL; Maliki et al. 2000) are also plotted on the same

diagram. The equations describing the relationship between the $\delta^{18}\text{O}$ and $\delta^2\text{H}$ values are the following:

$$\text{GMWL} : \delta\text{D} = 8 \times \delta^{18}\text{O} + 10 \quad (1)$$

$$\text{LMWL} : \delta\text{D} = 8 \times \delta^{18}\text{O} + 13.5 \quad (2)$$

The relatively high value of the deuterium excess (d), 13.5, reflects the participation of condensing vapor of Mediterranean air masses (Maliki 2000). The points representing the groundwater, when plotted on the $\delta^2\text{H}$ - $\delta^{18}\text{O}$ diagram, define a regression line: $\delta\text{D} = 4.01 \times \delta^{18}\text{O} - 13.62$. The value of the slope, 4.01, is lower than the slope of the GMWL (8), demonstrating that the groundwater experienced the evaporation effect, which produces isotopic enrichment of the surface water through the unsaturated zone or on surface before infiltration. Indeed, the deuterium intercept value (-13.62) is substantially lower than 10, confirming the evaporated aspect of the water before infiltration. This significant rate of evaporation in the study area is chiefly linked to the aridity, which is characteristic of the North Africa climate. The points that show this phenomenon are those located below (or to the right of) the GMWL, and this group of groundwater samples comprises waters relatively enriched in stable isotope contents with respect to the GMWL. In the investigated area, the long-term flood

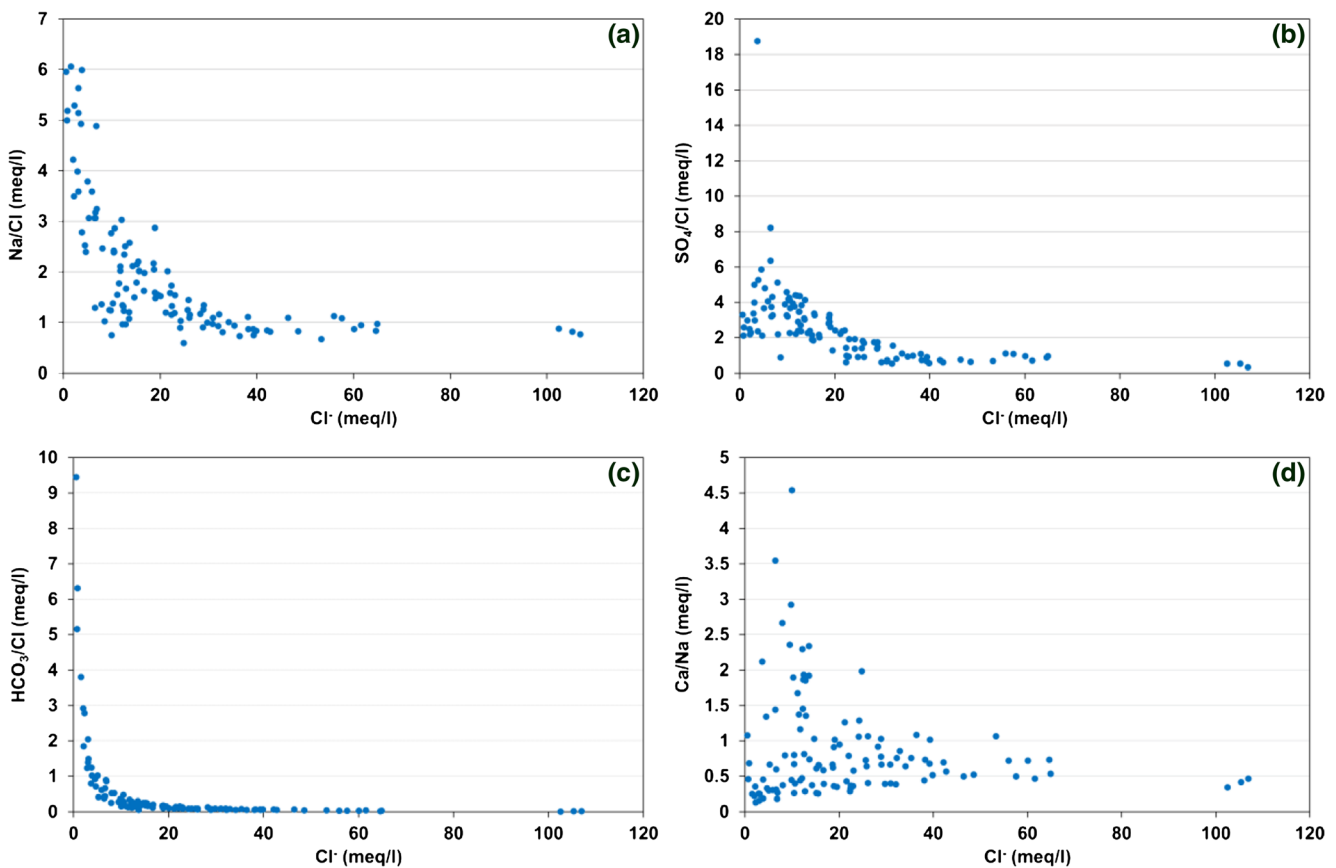


Fig. 9 Relationship between **a** Cl and Na/Cl; **b** Cl and SO₄/Cl; **c** Cl and HCO₃/Cl; **d** Cl and Ca/Na

irrigation practices have created favorable conditions for the isotopic fractionation of water before infiltration related to partial evaporation. Additionally, partial evaporation at the water table cannot be excluded due to the aridity of the climate, especially when the well/borehole depths are restricted. The water samples Nos. 17, 18, 20, 21, 23, 26, 32, 45, 74, 79, 87, 89, 91, 92, 98, 99, 100, 101, 102, 103, 104, 105 and 108 are scattered between the GMWL and the LMWL. The deuterium excess values for these water samples (22% of all groundwaters) include the range from 10‰ for global precipitation to 14‰ for the western Mediterranean area indicating the significance of the Mediterranean as a moisture source for the study area. This second group of groundwater indicates that the precipitation responsible for the recharge of the Sfax aquifer may have originated from a mixture of oceanic and Mediterranean vapor masses (Celle-jeanton et al. 2001; Montoroi et al. 2002). The similarity in isotopic composition between the groundwaters and local precipitation ($\delta^{18}\text{O}$: -4.6‰ VSMOW) indicates that they are not significantly affected by evaporation, implying direct recharge by rapid infiltration of rainwater. On the contrary, almost all groundwater samples showing low *d*-excess values suggest the participation of Atlantic air masses (*d*-excess = 10‰). The third group is composed of several groundwater samples (Nos. 52, 53, 55, 56, 63, 80, 84, 93, 94, 96, 97, 106, 111 and 116), located particularly in the Northwestern parts of the basin, that plot on the extreme left side,

revealing a relative depletion in their isotope contents ($\delta^{18}\text{O}$ values vary between -5.76 and -6.86‰), probably due to mixing with old groundwater through a leakage process. The mixing process suggests an upward leakage flow from the deep Miocene groundwater into the shallowest Miocene-Quaternary aquifers (Ayadi et al. 2016). The upward leakage of the deep aquifer is confirmed by the mixing proportion calculations, in which the contribution to the intermediate aquifer can reach 100% in the northwestern part of the basin (Ayadi et al. 2016). These groundwaters were probably recharged under different climatic conditions than the present day. The presence of an old component is supported by the radiogenic ^3H analyses, as low or undetectable ^3H contents were measured in some samples (0 TU in well Nos. 52 and 53; 0.12 TU in well No. 56; 0 TU in well No. 97), which implies an absence of recent water infiltration. The values of the deuterium excess (*d*) of the groundwater samples, which are indicative of the origin of the vapor masses generating the precipitation, were calculated using the following equation:

$$d = \delta\text{D} - 8 \times \delta^{18}\text{O} \quad (3)$$

The relationship between the $\delta^{18}\text{O}$ and $\delta^2\text{H}$ values in the groundwater samples differs in both the slope and the deuterium excess compared to the global and local meteoric water lines. The calculated *d* values in the study area vary

Table 3 Isotope composition, deuterium excess (d_{excess}) values and calculated recharge elevations (ΔZ)

Site/sample No.	Sample name	^2H (‰ vs SMOW)	^{18}O (‰ vs SMOW)	d_{excess} (‰)	ΔZ (m a.s.l.)	^3H (TU)	^{14}C (pmc)
1	Hafedh Jarraya 1	-28.34	-3.68	1.11	–	1.85	–
2	Hafedh Jarraya 3	-30.45	-4.48	5.37	–	–	–
3	Med Chabchoub 1	-34.49	-4.97	5.26	–	1.21	47.00
4	Med Chabchoub 2	-34.07	-4.45	1.50	–	–	–
5	Mahdi Jarraya	-34.56	-4.28	-0.30	–	–	–
6	Nabiha Charfi	-34.43	-4.49	1.49	–	0.75	–
7	OTD Essalema	-36.81	-4.83	1.80	–	–	–
8	Tarak Fourati	-37.59	-4.73	0.28	–	–	–
9	Zied Fourati 2	-35.27	-4.48	0.59	–	0.60	–
10	Emma Fourati2	-35.88	-4.87	3.09	–	–	–
11	Zied Fourati 3	-34.45	-4.22	-0.70	–	–	–
12	Hafedh Jarraya 2004 (attoura)	-37.72	-4.61	-0.81	–	–	–
13	Med Dziri	-23.50	-3.36	3.35	–	–	–
14	Nasr Eddeli	-26.65	-4.22	7.08	–	0.86	–
15	Forage PF 83	-36.59	-5.18	4.84	193	0.65	–
16	Forage PF 100	-35.03	-5.07	5.52	156	–	–
17	Chaal 1	-31.04	-5.34	11.65	245	3.35	–
18	Forage Nejah haj Ltaief	-32.24	-5.26	9.81	218	0.87	–
19	F. Mourad Ellili	-33.87	-4.95	5.69	–	–	–
20	F. mostfa belhaj ltaief	-31.77	-5.55	12.66	318	4.27	–
21	Ahmed Zribi	-34.00	-5.37	8.98	258	0.20	–
22	Ali Chouket	-37.06	-5.57	7.54	325	0.97	–
23	Sahbi Jirjir	-33.51	-5.56	11.00	321	2.28	–
24	Mohamed Zribi (2010)	-32.54	-4.84	6.16	–	0.00	–
25	Abdellatif Frikha	-34.90	-5.38	8.12	260	1.01	–
26	Forage Nabiha Kolsi	-32.56	-5.65	12.65	–	0.47	76.00
27	F. Ali B.Salem	-35.97	-5.13	5.06	176	1.30	–
28	F. Med Khaled Ellouze	-37.38	-5.19	4.16	197	–	29.00
29	F. Ali Abouda	-38.90	-5.42	4.50	275	0.73	–
30	F. Jilani Ltaief	-38.34	-5.17	2.99	189	–	21.20
31	F. Moez Mezghani	-35.26	-5.40	7.91	265	0.47	56.70
32	F. Abdelhafith Bougueffia	-33.48	-5.32	9.06	239	–	58.00
33	F. Limaya	-34.47	-4.84	4.25	–	–	–
34	Mourad Nouri	-36.40	-5.47	7.40	–	0.68	55.00
35	F. Haj Gacem	-38.23	-5.03	2.02	291	1.36	–
36	Othmen Maalej 1	-26.07	-4.39	9.02	144	–	–
37	Othmen Maalej 2	-35.93	-4.89	3.18	–	1.04	–
38	Ltaif Mezghanni	-37.73	-4.96	1.93	–	0.20	–
39	Zouhir Mziou 1	-35.79	-5.18	5.63	192	0.60	–
40	Zouhir Mziou 2	-36.38	-5.57	8.14	–	–	–
41	Mustapha Frikha (1) 2013	–	–	–	–	–	–
42	Mustapha Frikha (2) 2013	–	–	–	–	0.49	–
43	Sfax Zeliana	-36.86	-5.17	4.54	192	0.67	–
44	Hedi Ellouze	-30.73	-4.72	7.04	–	0.20	–
45	Mahmoud Mezghanni	-27.27	-4.77	10.92	58	0.95	–
46	Hsan Maktouf	-22.38	-2.97	1.37	–	0.00	–
47	Tarek Hammemi	-32.59	-3.47	-4.84	–	0.26	–
48	F. Hmed Mlawah	-29.23	-3.91	2.08	–	–	–
49	F.Med Adwani	-27.59	-4.02	4.55	–	1.04	–
50	F.Jarbouii	-27.56	-3.76	2.52	–	0.50	–
51	F.Merkez Kammoun	-30.07	-3.95	1.53	–	0.18	–
52	Khlifa Gdarat	-34.06	-6.17	15.29	–	0.00	–
53	TaherRahal	-33.24	-6.14	15.86	–	0.00	–
54	Med Masmoudi	-33.62	-5.28	8.63	227	0.00	–
55	CFJR	-44.18	-6.86	10.71	–	1.07	–
56	Hafedh Jarraya (Ksar Irrih)	-38.12	-6.30	12.28	–	0.12	–
57	Mustapha Frikha No. 1	–	–	–	–	–	12.70
58	Jamel Laarif	-33.49	-5.37	9.51	258	0.21	–
59	Khalil Ennouri	-37.51	-5.04	2.78	145	–	–
60	Mohamed Ben Omor	-32.01	-4.64	5.11	–	0.25	–
61	Hamada	-32.32	-5.07	8.26	158	–	10.40
62	Henchir Gara	-32.60	-4.90	6.61	–	1.56	–
63	Fawzi Mseddi	-40.14	-5.76	5.94	–	–	15.50
64	Forage Agareb	–	–	–	–	–	–
65	F. Neila Eleuch (debut de l'essai)	-37.71	-5.04	2.64	148	–	–

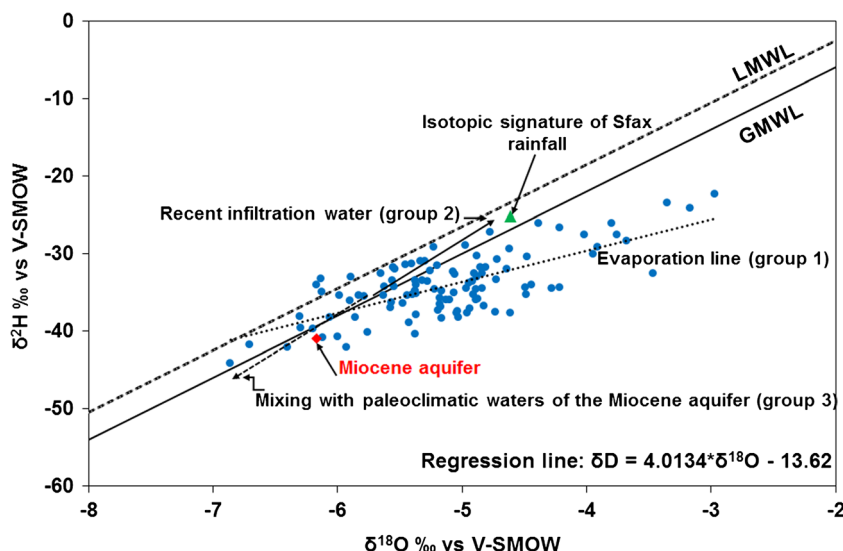
Table 3 (continued)

Site/sample No.	Sample name	^2H (‰ vs SMOW)	^{18}O (‰ vs SMOW)	d_{excess} (‰)	ΔZ (m a.s.l.)	^3H (TU)	^{14}C (pmc)
66	F. Neila Eleuch (fin de l'essai)	-37.90	-5.37	5.06	256	–	–
67	Gargouri Anouar	–	–	–	–	–	2.80
68	Mohamed Eddib	-34.89	-5.17	6.45	189	1.04	–
69	Noamen Mhadbi	-30.32	-4.89	8.76	95	0.60	–
70	Mbarek Neyli	-34.91	-5.38	8.11	–	0.40	–
71	Omor Ben Salah	-31.77	-4.85	7.05	–	0.75	39.00
72	Mongi Ben chibéni	-33.65	-4.92	5.69	–	0.98	–
73	Mohamed Kthiri	–	–	–	–	0.55	–
74	Hédi Démi	-28.90	-4.97	10.87	124	0.55	17.10
75	Mohsen Mayeh	-34.60	-5.22	7.20	208	0.93	–
76	Khalifa Lazzez	-33.37	-4.73	4.46	–	0.55	–
77	Ferjani yamina	-35.96	-5.10	4.84	–	0.40	3.60
78	Moncef Gdoura	–	–	–	–	–	–
79	Mahdi Trabelsi	-31.60	-5.20	10.00	200	–	–
80	Fawzi Msidi 2	-40.80	-6.00	7.20	–	–	–
81	Chaal 7 bis	-34.98	-6.13	14.06	–	0.00	–
82	Fraj Ghribi	-26.10	-3.80	4.30	–	–	–
83	Rajab El Hedi	-35.45	-5.44	8.07	–	–	–
84	Sofiene Kallel	-40.93	-6.12	8.05	–	–	–
85	Med Chabchoub 3	-29.43	-4.62	7.54	–	0.00	–
86	Mouldi Bilayedi Ben Ali	-40.38	-5.38	2.63	–	–	–
87	Hamad Belhaj Ltaief	-35.38	-5.83	11.26	–	2.53	–
88	Aboufa Zribi	-32.64	-5.06	7.85	154	1.24	–
89	Forage Taoula (Zribi)	-36.09	-5.90	11.10	–	1.15	–
90	Abdelkader Belhaj Ltaief	-33.09	-4.88	5.95	–	–	–
91	Mohamed Ben Nasr	-35.52	-5.79	10.78	–	–	–
92	Noemen Belhaj Ltaief	-33.02	-5.90	14.15	–	4.76	–
93	Salah Oued Rkham	-39.58	-6.29	10.78	–	–	–
94	Belgacem Fatnassi	-42.16	-5.93	5.25	–	1.07	–
95	Belgacem Mabrouki	–	–	–	–	–	–
96	BelgasseM Mabrouki No. 2	-39.70	-6.20	9.90	–	–	–
97	BelgasseM Mabrouki No. 3	-41.75	-6.71	11.93	–	0.00	–
98	Mounir El ghali	-31.50	-5.46	12.15	285	0.77	–
99	Naceur ben Ali	-35.42	-5.63	9.62	–	–	–
100	Salem Baccouche	-31.98	-5.54	12.31	312	0.00	–
101	Hakim Bouzayene	-35.39	-5.99	12.51	–	–	–
102	Forage Hzag	-31.39	-5.41	11.87	269	0.61	–
103	Naceur Thkir	-34.24	-5.63	10.77	–	–	–
104	Med Mansouri	-29.14	-5.23	12.71	210	0.39	–
105	Med Maaoui	-30.99	-5.30	11.42	234	–	–
106	Sté El Itha (Abdelaziz Makhloufi)	-42.10	-6.40	9.10	–	–	–
107	Forage Rami	–	–	–	–	–	–
108	Sadok Rwag (AGIL)	-34.27	-5.55	10.13	–	–	–
109	Bechir Haj Ltaief	-35.24	-5.37	7.72	–	–	–
110	Amor Mezghanni	-35.26	-4.91	4.02	–	–	–
111	Amor Mezghanni (Societe el baraka)	-38.21	-6.06	10.27	–	–	–
112	Mustapha Frikha 2	-37.12	-4.94	2.40	–	–	–
113	Jamil Triki	-24.21	-3.17	1.15	–	–	–
114	Abdel Majid Ben Mansour	-34.58	-4.89	4.54	–	–	–
115	Fakhreddine Ben Kridis	-31.76	-4.81	6.72	–	–	–
116	Lazhar Bali	-38.29	-5.86	8.59	–	–	–

within a range of -4.84 ‰ in sample No. 47 to $+15.86$ ‰ in sample No. 53 (Fig. 11; Table 3). Some of these values fall within the range between 10 (global precipitation) and 13.5 (the local precipitation), indicating the significance of the local rainfall as a moisture source for Sfax. However, most of the groundwater samples have low deuterium excess values (below 10 ‰), suggesting that the groundwater was recharged from precipitation that experienced strong evaporation during its fall or on the surface (Fig. 11). This

indicates that the majority of the samples that form this line experienced evaporation and/or mixed with evaporated water, which explains the increase in the stable isotope contents of this group of water. Furthermore, several groundwater samples with the lowest d values (from -4.84 to 2.99 ‰) are isotopically more enriched, recording a stronger evaporation effect. This may be related to climate aridity but may also be related to the depth and duration of the water–rock interaction during water infiltration,

Fig. 10 The $\delta^2\text{H}/\delta^{18}\text{O}$ diagram of the groundwater



which would suggest strong mineralization. A *d* value of approximately 10 ‰ indicates that the water has not been significantly evaporated, and plots on the GMWL and close to the LMWL. The water samples that plot below the GMWL show low deuterium excess values (< 10‰), indicating that the groundwater is isotopically different from its original isotopic composition due to evaporation. To locate the isotopic contents of the groundwater points in the regional isotopic context, local variations with altitude should be considered. This relationship, based on the thermal dependence of stable isotope contents, leads to the interpretation that when altitude increases, the isotopic contents are increasingly depleted as the average air temperature becomes lower. For the $\delta^{18}\text{O}$ altitudinal gradient (*G*), a depletion varies from -0.15 to -0.5 ‰ /100 m, corresponding to a deuterium depletion of -1 to -4 ‰ /100 m (Clark and Fritz 1997). The estimated aquifer recharge

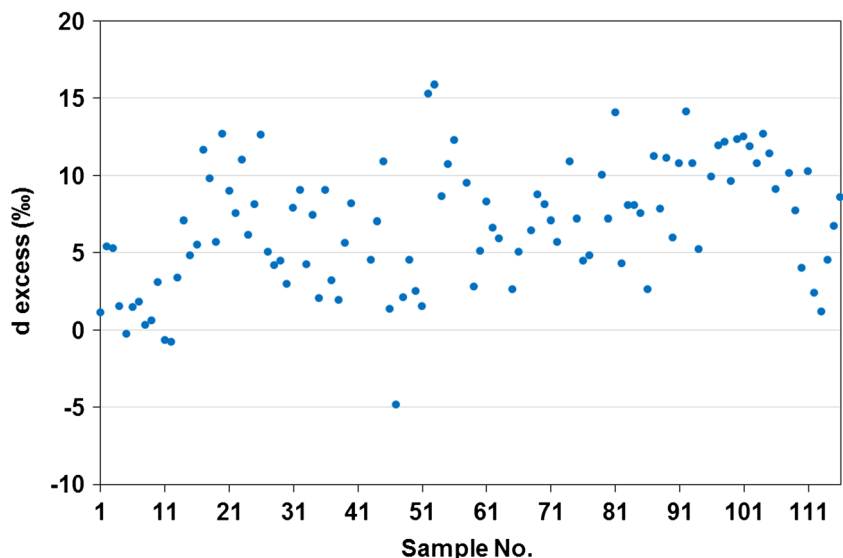
altitude (ΔZ) varying between 58 and 325 m.a.s.l (Table 3) are calculated using the following equation:

$$\Delta Z = 100 \times (\delta^{18}\text{O}_{\text{groundwater}} - \delta^{18}\text{O}_{\text{WMPS}}) / G \quad (4)$$

The theoretical $\delta^{18}\text{O}$ gradient is about 0.3 ‰ per 100 m ($G = 0.3$; Zuppi et al. 1974; Blavoux 1978; Maliki et al. 2000); the $\delta^{18}\text{O}$ of the weighted mean precipitation in Sfax station (WMPS) is -4.6 ‰ VSMOW.

Groundwater samples showing very high ΔZ values are relatively more depleted in stable isotope contents than the weighted mean values of $\delta^{18}\text{O}$ and $\delta^2\text{H}$ observed at the Sfax station. This in turn suggests that this water group has been recharged at altitudes higher than the elevation of the local rainfall station (10 m a.s.l.). The calculated values coincide with the elevation of the aquifer outcrops in the study area. This calculation pattern excludes

Fig. 11 Plot of deuterium excess (*d* excess) values of water samples



significantly depleted and enriched groundwater samples, affected either by paleoclimatic effect and/or by recent evaporated effect, respectively. The distribution of the $\delta^{18}\text{O}$ values of sampled waters shows a remarkably gradual decrease with increasing recharge elevation (Fig. 12). The lowest recharge elevations are found in samples Nos. 45, 69 and 74, located in Bir Ali Ben Khalifa and Skhira regions, for which $\delta^{18}\text{O}$ content is lower than -5‰ VSMOW. The recent infiltrated water is confirmed by tritium contents observed in these samples (F45: 0.95 TU; F69: 0.60 TU; F74: 0.55 TU), located in Bir Ali Ben Khalifa (F45) and Skhira (F69 and F74) regions. However, the highest elevation values are measured in the samples Nos. 20, 22, 23 and 100 (Table 3), which are relatively more depleted in ^{18}O and ^2H contents ($\delta^{18}\text{O} > -5.5\text{‰}$ VSMOW) and are particularly located in Bir Ali Ben Khalifa, the western part of Sfax. The outcrops of Bir Ali Ben Khalifa and Menzel Chaker constitute the recharge areas of the aquifer. The samples—Nos. 52, 53, 55, 87, 88, 89, 90, 91 and 92—are characterized by low TDS concentrations ($< 2,000$ mg/L), indicating low mineralization/short residence time and short groundwater flow paths (Table 2). In contrast, sample No. 56 (depth: 180 m), depleted in both ^{18}O and ^2H contents, shows the highest TDS concentration (TDS: 8,852.7 mg/L), which may be related to the enhanced water–rock interaction along the groundwater flow path, leading to halite dissolution (Na-Cl-SO₄ water type) and a long residence time (Mg/Ca ~ 1). The evaporate minerals dissolution would explain its high mineralization, and the slow water infiltration through the low transmissivities of the saturated zone layers would explain the long groundwater residence time. Based on the isotopic gradients, the recharge areas in the study area are located mainly in the north-western part of the basin, and water infiltrates via direct infiltration, which indicates enhanced interaction with the permeable layers of sandstones and clayey sands located in this area. These findings suggest short groundwater flow paths, short residence times (Mg/Ca ~ 0.66) and low TDS concentrations ($< 2,000$ mg/L). This pattern is supported by the measured tritium

contents of the analyzed samples in this area. The ^3H values range from 0.00 to 4.76 TU (Table 3), indicating the presence of local modern recharge in the groundwater from the intermediate aquifer. However, some groundwater samples have low or undetectable ^3H concentrations (< 0.5 TU), which are indicative of the absence of recent water infiltration. These low values are found particularly in water samples from great depths and from zones of low transmissivity in the aquifer formations that contribute to slower water infiltration in the saturated zone. This pattern is also observed in several samples located in the coastal areas of Djebeniana and Skhira towards the Mediterranean Sea (discharge area). The absence of ^3H concentrations in samples located near the coast could be related to long groundwater flow paths (long residence time) and/or a mixture with groundwater that formed under past climate conditions.

Carbon isotope content and groundwater age dating

Tritium is a dating isotope of young waters. The occurrence of tritium in groundwater indicates the extent of migration of modern post-1950s recharge. Its short half-life of about 12.43 years does not provide an exact dating for the old waters. In this case, the radiocarbon isotope is used as an excellent tracer for groundwaters with medium and long residence time. The groundwater dating by the radiocarbon isotope is conjoined with the ^3H contents, to confirm the groundwater age via old/recent waters. Radiocarbon allows the determination of water residence time over timescales to 30 ka (Clark and Fritz 1997).

The evolution of groundwater in the intermediate aquifer has been described for an area that is completely arid today but which is known from past climatic records to have been wetter in the late Pleistocene and Holocene. The radiocarbon activity has been determined for 14 boreholes and shows data within a range of 2.8–76 pmc (Fig. 13; Table. 3), indicating the complexity of the groundwater dynamics. These data can be used to classify the groundwater into different groundwater

Fig. 12 Plot of $\delta^{18}\text{O}$ values of analyzed water samples versus aquifer recharge altitude (ΔZ)

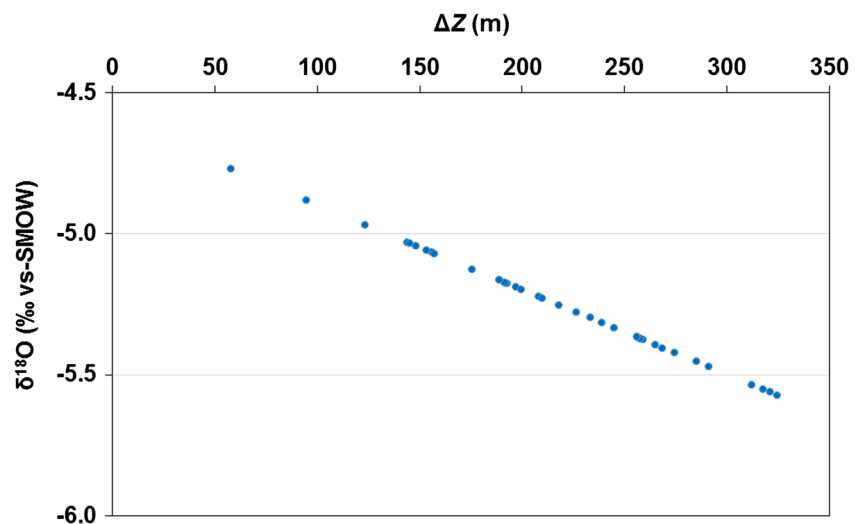
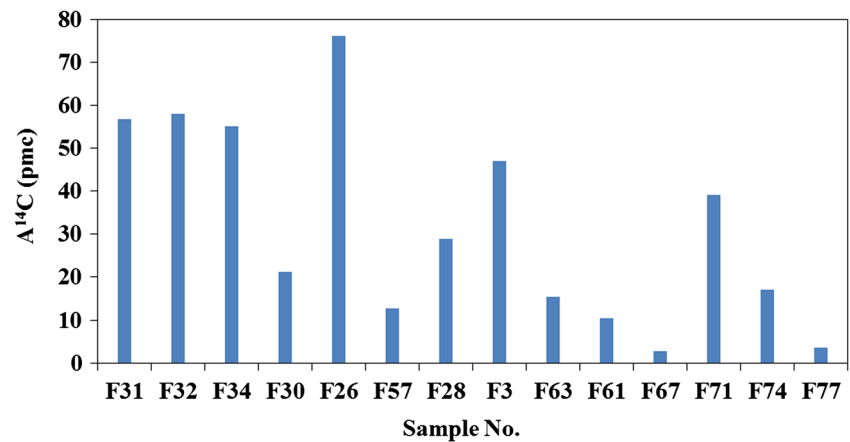


Fig. 13 Radiocarbon activities of the groundwater samples



recharge periods, indicating old and young groundwaters. The groundwater isotopic evidence in different places records strong variations in the humidity of the air masses supplying moisture across the continent at different times over the past 30,000 years. Similar to the relationships between carbon-14 (%) and infiltration period (age) plotted by several authors for the Saharan platform and North Africa (Edmunds et al. 1997; Guendouz et al. 2003), the $\delta^{18}\text{O}$ data (‰) are plotted vs. computed age, years Before Present (BP), for the groundwater samples in the study area (Fig. 14). Most of the samples (21.2–58 pmc) correspond to a Holocene recharge period. Three samples (No. 61, $\delta^{18}\text{O}$: -5.07 ‰; No. 74, $\delta^{18}\text{O}$: -4.97 ‰; and No. 77, $\delta^{18}\text{O}$: -5.10 ‰), located in the southern coastal area of the basin (Skhira area) correspond to the late Pleistocene period. In contrast, a younger water sample (No. 26) with a high radiocarbon activity of 76 pmc, located in the western study area, corresponds to modern recharge (-5.65 ‰; Fig. 14). The $\delta^{13}\text{C}$ analyses carried out was in the TDIC range from -11.01 to -8.04 ‰ (Table 4). Seven correction models based on the chemical evolution and/or isotope

dilution of $^{13}\text{C}/^{12}\text{C}$ derived from soil CO_2 through interactions with aquifer carbonates were adopted to estimate the groundwater age. It is highlighted that ages proposed by Ingerson and Pearson (1964), Evans et al. (1979), Eichinger (Eichinger 1983) and Fontes and Garnier (1979) are globally in good agreement and provide very similar ages. The models of the International Atomic Energy Agency (IAEA; Salem et al. 1980) and Tamers (1975) suggest greater ages than the previous models. The Mook models (Mook 1980) tend to give rise to over-estimations of groundwater residence times. The ^{14}C activities were corrected using the Pearson model. The computed ages varies from the actual to 21,000 years BP. These results confirm the complexity of the recharge process inferred from stable isotopes and chemical analysis. These data can classify the groundwaters into three groups: (1) ages between modern and 3000 years BP corresponding to local recent infiltrated waters; (2) ages between 4500 and 10,000 years BP, such as F61 and F74, which indicates the relatively old origin of the water, resulting from the long groundwater flow path probably linked to the low permeability of the sandy clay levels, and/or

Fig. 14 The computed age/ $\delta^{18}\text{O}$ relationship

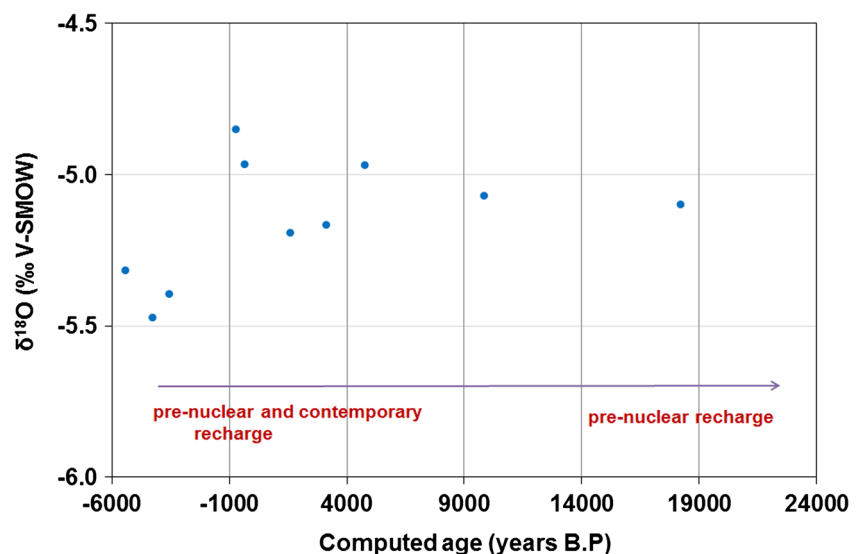


Table 4 Calculated ages of selected groundwater samples. Ages are expressed in years Before Present (BP)

Site/sample No.	¹⁴ C (pcm)	¹³ C (‰)	¹³ C _{Gaz. Eq.} (‰)	Age Brut	Age Tamers	Age Pearson	Age Mook	Age F. & G.	Age AIEA	Age Evans	Age Eichinger
F31	56.7	-9.39	-19.9	4,690	Actual	Actual	11,154	Actual	2,942	Actual	Actual
F32	58	-8.04	-18.2	4,503	Actual	Actual	13,909	Actual	1,087	Actual	Actual
F34	55	-8.58	-19.0	4,942	Actual	Actual	13,227	Actual	2,234	Actual	Actual
F30	21.2	-8.21	-18.7	12,823	7,324	3,155	21,498	3,258	9,637	3,501	2,854
F26	76	-	-	2,269	-	-	-	-	-	-	-
F57	12.7	-	-9.5	17,059	12,248	-	34,385	-	-	-	-
F28	29	-9.06	-13.4	10,233	7,342	1,625	-	1272	5,962	964	Actual
F3	47	-11.01	-17.8	6,242	1,847	Actual	-	Actual	4,181	Actual	Actual
F63	15.5	-	1.2	15,412	15,412	-	37,017	-	-	-	-
F61	10.4	-8.86	-16.0	18,710	13,768	9,865	-	9,640	14,127	9,127	9,168
F67	2.8	-9.04	-7.9	29,558	29,558	20,926	47,200	21,215	27,409	21,215	-
F60	39	-9.16	-18.8	7,784	2,856	Actual	16,205	Actual	5,775	Actual	Actual
F74	17.1	-8.09	-17.8	14,600	9,611	4,770	24,553	4,896	11,252	5,126	3,972
F77	3.6	-8.54	-18.7	27,480	22,202	18,240	36,110	18,337	24,722	18,562	17,756

from a mixture with old water coming from the Miocene deep groundwater; and (3) the greatest ages (> 10,000 years BP) that support the paleoclimatic origin of groundwaters. This water group (samples Nos. 67 and 77) has been recharged under colder climatic conditions than the present day, during the late Pleistocene. This is consistent with negligible radiocarbon and tritium content (F67: 2.8 pcm and F77: 3.6 pcm; 0.4 TU). The depleted isotopic signature of the majority of water samples shows that the groundwater was recharged under distinctly different climatic conditions, during late Pleistocene and early Holocene (Fig. 14).

It is evident from Fig. 15 that the spatial patterns of mean residence time and ¹⁴C activity in the Mio-Pliocene groundwater do not follow a unique flow path. The groundwater characterized by the Na-SO₄ water type (sample No. 26)

presents a short residence time (age: 2269 years BP), ¹⁴C = 76 pcm and ³H = 0.47 TU. From this information, it is apparent that this groundwater sample is composed of a recent water component. This is in agreement with the δ¹⁸O/δ²H diagram, which shows that the sample is located between the meteoric water lines (with *d* = 12.65 ‰), indicating recent local recharge. In contrast, the groundwater characterized by the Ca-Na-SO₄ water type (sample No. 28) presents a relatively long residence time (9948 years BP), depth = 145 m and ¹⁴C = 29 pcm. These data imply that this water may be attributed to pre-nuclear recharge and/or a mixture between pre-nuclear and contemporaneous recharge. This water sample was recharged in association with evaporation (*d* = 4.16 ‰) that occurred during its infiltration through sandy clayey and evaporitic levels that resulted in a high TDS concentration (5,293 mg/L

Fig. 15 The ¹⁴C/TDS relationship

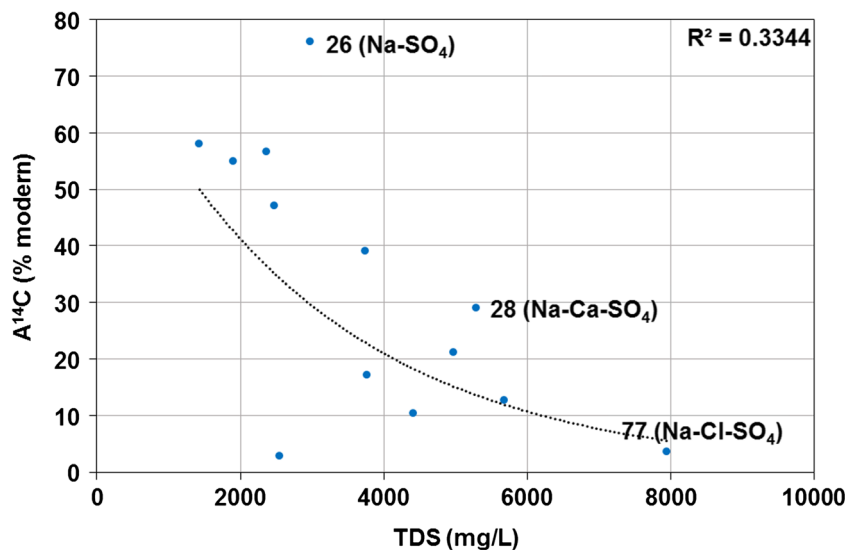
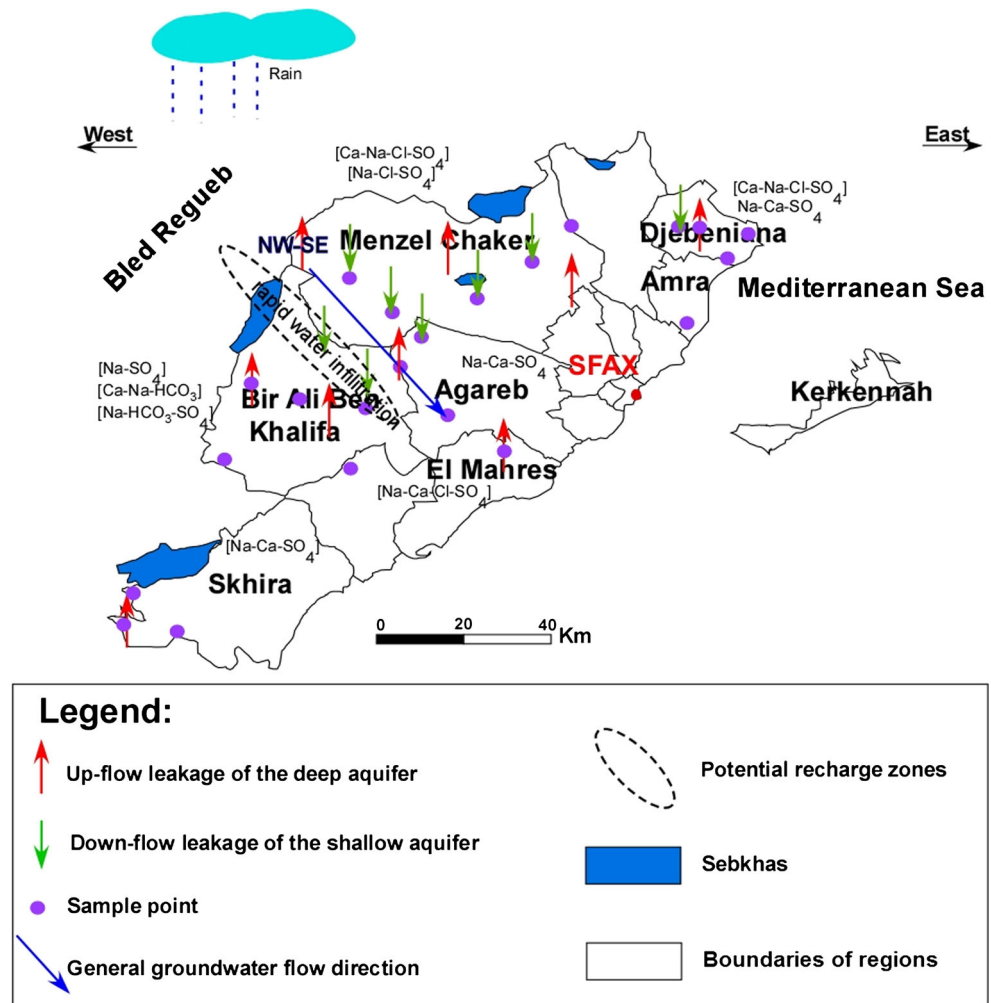


Fig. 16 Conceptual groundwater dynamics model showing the vertical leakage process contributing to the recharge of the intermediate aquifer in Sfax basin



L) and a relatively prolonged groundwater residence time. Furthermore, the groundwater characterized by the Na-Cl-SO₄ water type (sample No. 77) presents a longer residence time with ¹⁴C = 3.6% and a high TDS value of 7,952 mg/L. The low ¹⁴C content measured in this sample, located in the southern coastal part of Sfax, can be explained by the long groundwater flow path due to the dominance of evaporitic deposits. This water sample was affected by evaporation (*d* = 4.84 ‰). Slower infiltration through the clayey layers, which are interbedded with sandstones, contribute to delay the water infiltration in the unsaturated zone and to increase the groundwater residence time. The groundwaters show a geochemical evolution between Ca-Na-SO₄, Na-SO₄ and Na-Cl-SO₄ water types. The dominance of SO₄-Na and Cl ions probably indicates prolonged water infiltration within the intermediate aquifer due to the low transmissivities of the evaporitic and clayey aquifer formations, that contribute to a prolonged and longer groundwater flow path, i.e., mainly evaporitic rock dissolution, evaporation and cation exchange, which can successfully explain the observed changes in HCO₃ and TDIC. The groundwater dynamics and the leakage

process contributing to the recharge of the intermediate aquifer (Fig. 16) is confirmed by the isotope mass balance calculations (Ayadi et al. 2016), indicating interaction between the different Sfax aquifer layers. This provides evidence that the groundwater has recharged during large-scale periods with variability in recharge mechanisms that lead to variation in the groundwater residence times, supported by the carbon-14 contents.

Conclusions

The geochemistry and isotope hydrology of the groundwater in the intermediate aquifer of the Sfax basin (southeastern Tunisia) have provided useful insights into the water types, mineralization processes, origins, recharge mechanisms and residence times. This detailed investigation is of a particular importance for sustainable management of these groundwater resources, especially in arid zones coupled with the increasing exploitation for irrigation and domestic supply.

The chemical data showed significant variations in salinity and evolution in the hydrochemical facies that could be related to the facies changes in the geological formations of the studied zone and the tectonic activity. The water chemistry of the studied groundwater is chiefly governed by several processes: (1) the dissolution of evaporitic minerals, (2) cation exchange reactions caused by the interaction with clay minerals, and (3) mixing processes. The stable isotope data indicate that the groundwater samples are mostly of a meteoric origin and are derived mainly from oceanic vapor masses. These isotopic tracers reveal the existence of three groups of water: (1) non-evaporated groundwater, suggesting rapid infiltration of unevaporated recharge water, (2) evaporated waters, defined by an evaporation-driven deviation from the meteoric lines and characterized by an enrichment in heavy isotopes, suggesting the occurrence of partial evaporation at the surface prior to, during, or after infiltration through the unsaturated zone or mixing with evaporated infiltrated water, and (3) mixed water composed of recent and old components, depleted in oxygen-18 and deuterium. The radiogenic (^3H) isotope data indicate significant evolution in the groundwater in terms of old versus recent recharge. These data provide evidence that the groundwater in the intermediate aquifer represents a bimodal system: recent groundwater ($^3\text{H} > 1 \text{ TU}$), which involves modern recharge supplied by a direct and rapid floodwater infiltration (mainly recorded in the western and northwestern parts of the basin), and old groundwater ($^3\text{H} < 1 \text{ TU}$). Low tritium contents may indicate recharge prior to 1952 and/or a mixture between pre-nuclear and contemporaneous recharge. Carbon-14 activities versus $\delta^{13}\text{C}$ data provide evidence that most of the groundwater recharged during the Pleistocene and Holocene periods. The approaches used work towards better understanding of the groundwater dynamics and quality. They will constitute a useful tool to protect these important groundwater resources from declining and from salinization, by aiding managers to elaborate appropriate strategies for exploitation in further economic development of the Sfax region.

Acknowledgements We would like to thank the technical staff of the Laboratory of Radio-Analyses and Environment of the National Engineering School of Sfax (ENIS) for the chemical and isotopic analyses. Special thanks go to the staff members of Sfax Water Resources Division/Agriculture Ministry for the field work. We wish to thank the executive editor Clifford Voss, the editors, and the anonymous reviewers for their fruitful comments, which greatly helped to improve the paper.

References

- Aravena R, Wassenaar LI, Plummer LN (1995) Estimating ^{14}C groundwater ages in a methanogenic aquifer. *Water Resour Res* 31(9): 2307–2317
- Ayadi R (2017) Caractérisation hydrogéologique et géochimique de la nappe semi-profonde du système aquifère de Sfax [Hydrogeological and geochemical characterization of the intermediate aquifer of Sfax aquifer system]. PhD Thesis, Ecole Nationale d'Ingénieurs de Sfax, Tunisia, 216 pp
- Ayadi R, Zouari K, Saibi H, Trabelsi R, Khanfir H, Itoi R (2016) Determination of the origins and recharge rates of the Sfax aquifer system (southeastern Tunisia) using isotope tracers. *Environ Earth Sci J* 75(636). <https://doi.org/10.1007/s12665-016-5445-4>
- Belgacem A, Kharroubi A, Bouri S, Abida H (2010) Contribution of geostatistical modelling to mapping groundwater level and aquifer geometry: case study of Sfax's deep aquifer, Tunisia. *Middle East J Sci Res* 6(3):305–316
- Ben Ali R (2011) Contribution des approches hydrogéologique et hydrochimique à l'étude de la nappe semi profonde de Sfax [Contribution of the hydrogeological and hydrochemical approaches to study the intermediate aquifer of Sfax]. MSc Thesis, Faculty of Sciences of Sfax, Tunisia, 73 pp
- Ben Akacha M (2001) Etude géologique de la région d'Agareb-Sfax: évolution géomorphologique néotectonique et paléogéographique [Geological study of the Agareb-Sfax region: geomorphological, neotectonic and paleogeographic evolution]. DEA, Faculty of Sciences of Sfax, Tunisia, 94 pp
- Ben Brahim F, Bouri S, Khanfir H (2011) Hydrochemical analysis and evaluation of groundwater quality of a Mio-Plio-Quaternary aquifer system in an arid regions: case of El Hancha, Djebeniana and El Amra regions, Tunisia. *Arab J Geosci* 6:2089–2102. <https://doi.org/10.1007/s12517-011-0481-6>
- Beni Akhy R (1994) Evolution et modélisation de la nappe phréatique urbaine de Sfax [Evolution and modeling of the urban phreatic aquifer of Sfax]. Mémoire de DEA, Faculté des Sciences de Tunis, Tunis
- Blavoux B (1978) Etude du cycle de l'eau au moyen de l'oxygène 18 et du deutérium [Study of the water cycle using oxygen 18 and deuterium]. State Thesis, Université Paris VI, France, 316 pp
- Bouaziz S (1994) Etude de la tectonique cassante dans la plate-forme et l'Atlas Saharien (Tunisie méridionale): évolution des paléo-champs de contraintes et implication géodynamique [Study of brittle tectonics in the platform and the Saharian Atlas (Meridional Tunisia): evolution of the paleo-fields of constraints and geodynamic implication]. PhD Thesis, University of Sciences of Tunis II, Tunisia, 485 pp
- Bouchaou L, Michelot JL, Vengosh A, Hsissou Y, Qurtobi M, Gaye CB, Bullen TD, Zuppi GM (2008) Application of multiple isotopic and geochemical tracers for investigation of recharge, salinization, and residence time of water in the Souss-Massa aquifer, southwest of Morocco. *Hydrol J* 352:267–287
- Burrollet PE (1956) Contribution à l'étude Stratigraphique de la Tunisie Centrale [Contribution to the stratigraphic study of central Tunisia]. *Ann Min Géol* 18:345
- Castany G (1953) Les plissements quaternaires en Tunisie [The Quaternary folds in Tunisia]. *Comptes Rendus Sommaires Société Géologique de France, SGF, Paris*, pp 155–157
- Celle-Jeanton H, Zouari K, Travi Y, Daoud A (2001) Caractérisation isotopique des pluies en Tunisie: essai de typologie dans la région de Sfax [Isotopic characterization of rainfall in Tunisia: typology test in the Sfax region]. *CR Acad Sci Paris Sér IIA* 33:625–631
- Clark ID, Fritz P (1997) Environmental isotopes in hydrogeology. Lewis, Boca Raton, FL
- Coplen TB (1996) New guidelines for reporting stable hydrogen, carbon, and oxygen isotope-ratio data. *Geochim Cosmochim Acta* 60:3359–3360
- C.R.D.A (2015) Piézométrie des Nappes Aquifères du Gouvernorat de Sfax durant l'année 2014. *Annuaire d'exploitation des nappes aquifères de Sfax* [Piezometry of the aquifers of the Governorate of Sfax during the year 2014. Directories of exploitation of the aquifers of Sfax]. Commissariat Régionale d'Activité Agricole de Sfax, Sfax, Tunisia
- Craig H (1961) Isotopic variation in meteoric water. *Science* 133:1702–1703. <https://doi.org/10.1126/science.133.3465.1702>

- Custodio E (1987) Hydrogeochemistry and tracers. In: Custodio E (ed) Groundwater problems in coastal areas. Studies and Reports in Hydrology, vol 45. UNESCO, Paris, pp 213–269
- Dansgaard W (1964) Stable isotopes in precipitation. *Tellus* 16:436–438
- Edmunds WM, Guendouz AH, Mamou A, Moula A, Shand P, Zouari K (2003) Groundwater evolution in the continental Intercalaire aquifer of southern Algeria and Tunisia: trace element and isotope indicators. *Appl Geochem* 18:805–822
- Edmunds WM, Shand P, Guendouz AH, Moula A, Mamou A, Zouari K (1997) Recharge characteristics and groundwater quality of the Grand Erg oriental basin. Tech. Rep. WD/97/46R, British Geological Survey, Keyworth, UK
- Eichinger E (1983) A contribution to the interpretation of ^{14}C groundwater ages considering the example of partially confined sandstone aquifer. *Radiocarbon* 25:347–356
- El Batti J, Andrieux M (1977) Etude hydrogéologique et géophysique du secteur Wadrane [Hydrogeological and geophysical study of the Wadrane sector]. Internal report, DGRE, Tunis
- Evans GV, Otlet RL, Downing A, Monkhouse RA, Rae G (1979) Some problems in the interpretation of isotope measurements in United Kingdom aquifer. *Isotope Hydrol* 2:639–708
- Fedrigoni L, Krimissa M, Zouari K, Maliki A, Zuppi GM (2001) Origine de la minéralisation et comportement hydrogéochimique d'une nappe phréatique soumise à des contraintes naturelles et anthropiques sévères: exemple de la nappe de Djebeniana (Tunisie) [Origin of mineralization and hydrogeochemical behaviour of phreatic aquifer subjected to severe natural and anthropogenic constraints: example of the aquifer of Djebeniana (Tunisia)]. *Earth Planet Sci Lett* 332:665–671
- Fontes JC (1971) Un ensemble destiné à la mesure de l'activité du radiocarbone naturel par scintillation liquide [An assembly destined for measuring the activity of natural radiocarbon by liquid scintillation]. *Rev Geogr Phys Géol Dyn* 13(1):67–86
- Fontes JC, Garnier JM (1979) Determination of the initial ^{14}C activity of the total dissolved carbon: a review of the existing models and a new approach. *Water Resour Res* 15(2):399–413
- Gassara A, Ben Marzouk A (2009) Hydrogéologie de la nappe semi-profonde de Sfax [Hydrogeology of the intermediate aquifer of Sfax]. Report, CRDA., Sfax, Tunisia
- Guendouz A, Moulla AS, Edmunds WM, Zouari K, Shand P, Mamou A (2003) Hydrogeochemical and isotopic evolution of water in the complex terminal aquifer in the Algerian Sahara. *Hydrogeol J* 11: 483–495
- Hajjem A (1980) Etude hydrogéologique de la région de Sidi Abid [Hydrogeological study of the region of Sidi Abid]. Internal report, vol 8. DRES, Tunis
- Hao X, Change C (2002) Does long-term heavy cattle manure application increase salinity of a clay loam soil in semi-arid southern Alberta? *Agric Ecosys Environ* 193:4:1–16
- Hchaichi Z (2008) Etude hydrogéologique et géochimique de la nappe intermédiaire de Sfax et sa relation avec le système phréatique du bassin Nord de Sfax [Hydrogeological and geochemical study of the intermediate aquifer of Sfax and its relationship with the phreatic system of the Northern Sfax basin]. Mémoire de Mastère, Ecole Nationale d'Ingénieurs de Sfax (ENIS), Sfax, Tunisia, 116 pp
- Hchaichi Z, Abid K, Zouari K (2013) Use of hydrochemistry and environmental isotopes for assessment of groundwater resources in the intermediate aquifer of the Sfax basin (southern Tunisia). *Carbonates Evaporites* J. <https://doi.org/10.1007/s13146-013-0165-2>
- Hern J, Feltz HR (1998) Effects of irrigation on the environment of selected areas of the western United States and implications to world population growth and food production. *Environ Manag J* 52:353–360
- Ingerson E, Pearson FJ (1964) Estimation of age and rate of motion of groundwater by ^{14}C method. In: Miyake Y, Koyama T (eds) Recent researches in the fields of atmosphere, hydrosphere and nuclear geochemistry. Maruzen, Tokyo, pp 263–283
- Maliki A (2000) Etude hydrogéologique, hydrochimique et isotopique de la nappe profonde de Sfax (Tunisie) [Hydrogeological, hydrochemical and isotopic study of the deep aquifer of Sfax (Tunisia)]. PhD Thesis, ENIS, Tunisia
- Maliki A, Krimissa M, Michelot JL, Zouari K (2000) Relation entre nappes superficielles et aquifère profond dans le bassin de Sfax (Tunisie) [Relationship between superficial aquifers and deep aquifer in the Sfax basin (Tunisia)]. *Earth Planet Sci* 331:1–6
- Meybeck M (1987) Global chemical weathering of surficial rocks estimated from river dissolved loads. *Am J Sci* 287:401–428. <https://doi.org/10.2475/ajs.287.5.401>
- Montoroi JP, Grünberger O, Nasri S (2002) Groundwater geochemistry of a small hill reservoir catchment in central Tunisia. *Appl Geochem* 17:1047–1060
- Mook WG (1980) Carbone 14 in hydrogeological studies. In: Fritz P, Fontes JC (eds) The terrestrial environment. Handbook of Environmental Isotope Geochemistry, vol 1. Elsevier, Amsterdam, pp 49–74
- Parkhurst DL, Appelo CAJ (1999) User's guide to PHREEQC (version 2): a computer program for speciation, batch-reaction, one-dimensional transport, and inverse geochemical calculations. US Geol Surv Water Resour Invest Rep 99-4259
- Petalas CP, Diamantis IB (1999) Origin and distribution of saline groundwaters in the upper Miocene aquifer system, coastal Rhodope area, northeastern Greece. *Hydrogeol J* 7:305–316
- Plummer LN, Jones BF, Truesdell AH (1976) WATEQF, a FORTRAN IV version of WATEQ: a computer program for calculating chemical equilibrium of natural waters. US Geol Surv Water Res Invest 76-13:61
- Rahoui H, Koshel R (1980) Cartes des ressources en eau souterraine de la Tunisie à l'échelle de 1:200000 [Maps of groundwater resources in Tunisia at the scale of 1:200000]. Feuille de Sbeitla no. 14. Republic of Tunisia, Divisions des Ressources en Eau, Tunis
- Richter BC, Kreitler CW (1993) Geochemical techniques for identifying sources of ground water salinization. CRC, Boca Raton, FL
- Stuiver M, Polach H (1977) Reporting of ^{14}C data. *Radiocarbon* 19(3): 355–363
- Salem O, Visser JH, Dray M, Gonfiantini R (1980) Groundwater flow patterns in the western Libyan Arab Jamahiriya evaluated from isotopic data. In: Arid zone hydrology. Investigations with isotope techniques. International Atomic Energy Agency, Vienna (Austria), Panel proceedings series, pp 165–179
- Stumm W, Morgan JJ (1996) Chemical equilibria and rates in natural waters. Wiley, New York
- Takrouni M, Michelot JL, Maliki A, Zouari K (2003) Relation entre aquifère profond, nappes superficielles et intrusion marine dans le Bassin de Sfax (Tunisie) [Relationship between deep aquifer, superficial aquifers and marine intrusion in the Sfax basin (Tunisia)]. *Hydrol Mediterr Semiarid Reg* 278:1–7
- Tamers MA (1975) Validity of radiocarbon dates on groundwater. *Geophys Surv* 2:217–239
- Tayech B (1984) Etudes palynologiques dans le Néogène du Cap Bon (Tunisie) [Palynological studies in the Neogene of Cap Bon (Tunisia)]. PhD Thesis, Univ. Claude Bernard, Lyon I, France
- Taylor CB (1976) IAEA Isotope Hydrology Laboratory: technical procedure note no. 19. International Atomic Energy Agency, Vienna
- Trabelsi R, Zaïri M, Smida H, Ben Dhia H (2005) Salinisation des nappes côtières: cas de la nappe nord du Sahel de Sfax, Tunisie [Salinization of coastal aquifers: case of the northern Sahel water table of Sfax, Tunisia]. *CR Acad Sci Paris* 337:515–524
- Trabelsi N, Zaïri M, Triki I, Ben Dhia H (2006) Contribution du SIG à la gestion des ressources en eaux souterraines: Cas de la nappe profonde de Sfax, Tunisie [Contribution of GIS to the management of groundwater resources: case of the deep aquifer of Sfax, Tunisia]. Conférence francophone ESRI, Issy les Moulineaux, 2006
- Trabelsi R, Kacem A, Zouari K, Rozanski K (2009) Quantifying regional groundwater flow between continental Intercalaire and Djeferra

- aquifers in southern Tunisia using isotope methods. *Environ Geol* 58:171–183. <https://doi.org/10.1007/s00254-008-1503-x>
- Vengosh A (2003) Salinization and saline environments. In: Sherwood LB (ed) *Environmental geochemistry, treatise in Geochemistry*, vol 9. Elsevier, New York
- Vengosh A, Kloppmann W, Marie A, Livshitz Y, Gutierrez A, Banna M, Guerrot C, Pankratov I, Ranan H (2005) Sources of salinity and boron in the Gaza strip: natural contaminant flow in the southern Mediterranean coastal aquifer. *Water Resour Res* 41:W01013. <https://doi.org/10.1029/2004WR003344>
- Vengosh A, Hening S, Ganor J, Mayer B, Weyhenmeyer CE, Bullen TD, Paytan A (2007) New isotopic evidence for the origin of groundwater from the Nubian sandstone aquifer in the Negev, Israel. *Appl Geochem* 22:1052–1073
- Wen XH, Wu YQ, Wu J (2008) Hydrochemical characteristics of groundwater in the Zhangye Basin, northwestern China. *Environ Geol J* 55(8):1713–1724
- Yangui H, Zouari K, Trabelsi R, Rozanski K (2010) Recharge mode and mineralization of groundwater in a semi-arid region: Sidi Bouzid plain (central Tunisia). *Environ Earth Sci J* 63:969–979
- Zébidi H (1989) *Hydrogéologie de la nappe profonde de Sfax* [Hydrogeology of the deep aquifer of Sfax]. Report, DGRE, Tunis, 27 pp
- Zouari K, Trabelsi R, Chkir N (2011) Using geochemical indicators to investigate groundwater mixing and residence time in the aquifer system of Djefara of Medenine (southeastern Tunisia). *Hydrogeol J* 19:209–219. <https://doi.org/10.1007/s10040-010-0673-2>
- Zuppi GM, Fontes JCh, Letolle R (1974) Isotopes du milieu et circulation d'eaux sulfurées dans le Latium [Environmental isotopes and sulphurous water flow in the Latium]. In: *Isotope technique in ground water hydrology 1974* (Vienna, 11–15 March 1974), vol 1. International Atomic Energy Agency, Vienna, pp 341–361